

**INTERFACE SHEAR STRENGTH OF  
GEOMEMBRANES AND GEOTEXTILES AT  
DIFFERENT TEMPERATURES**

by

**MUHAMMET VEFA AKPINAR**

A thesis submitted in partial fulfillment of  
the requirements for the degree of

**MASTER OF SCIENCE  
(CIVIL AND ENVIRONMENTAL ENGINEERING)**

at the  
**UNIVERSITY OF WISCONSIN-MADISON**

**1997**

MEM  
AWO  
A3163  
M843

56 226 78

**INTERFACE SHEAR STRENGTH OF  
GEOMEMBRANES AND GEOTEXTILES AT  
DIFFERENT TEMPERATURES**

Approved :

 8/4/97  
.....  
Signature Date

Craig H. Benson, Associate Professor

## INTERFACE SHEAR STRENGTH OF GEOMEMBRANES AND GEOTEXTILES AT DIFFERENT TEMPERATURES

Muhammet V. Akpinar  
Under Supervision of Dr. Craig H. Benson  
at the University of Wisconsin- Madison

The objective of this study was to determine how temperature affects the interface strength between geotextiles and geomembranes. This objective was met by conducting shear tests at various temperatures using the Texas Double-Interface Shear Device.

A TDISD consists of an outer frame and an inner loading apparatus. Normal force was applied to the interfaces by applying air pressure to the piston. The base pedestal was raised at a constant rate of displacement using a loading frame. Shear displacement was measured with a LVDT (located on top of the box), and the shear force was measured with a load cell. A constant temperature box was designed to provide constant temperatures of 0°C, 10°C, 21°C, and 33°C during testing. The box was maintained at elevated temperatures using four lamps and a temperature controller with a thermocouple. Four fans circulated air within the box to ensure uniform temperature. Cooler temperatures (0°C and 10°C) were obtained by circulating cool air through the box via two tubes. One tube removed cold air from a refrigerator and blew the air into the box. The other tube evacuated air from inside the box and returned it to the refrigerator. Two thermometers were located between the specimens (on either side of the piston) to check the temperature. Testing began after thermal equilibrium was obtained.

The parameters varied in the testing program were temperature (0°C to 33°C), normal stress (15 to 49 kPa), and geosynthetic type (smooth HDPE geomembrane, textured HDPE geomembrane, and NWNP geotextile). Strain rates used in the tests were 0.15 cm/min, 0.11 cm/min, and 0.09 cm/min.

Results of the tests show that: (1) interface shear strength increases with increasing temperature. When the temperature conditions were increased from 0°C to 33°C the interface friction

angle increased for smooth gemembrane/NWNP geotextile and textured gemembrane/NWNP geotextile from 12° to 14° and from 25° to 27° respectively; (2) relaxation time has an effect on the interface friction angle. The friction angle obtained from tests conducted 6 hours after application of normal was 0.5° higher value than the friction angle obtained immediately after the constant set temperature was obtained, (3) for temperatures between 0°C and 33°C strain rate does not have a significant effect on interface shear strength, (4) the TDISD gives repeatable interface shear results when normal stresses are applied above 15 kPa. Below 15 kPa normal stress, the test is not reliable due to friction problems in the pistons, (5) the aluminum plates of the TDISD must be maintained parallel. Otherwise, misleading interface shear test results will be obtained.

## ACKNOWLEDGEMENT

I am indebted to my advisor, Professor C.H. Benson, for his guidance and assistance during this study and my coursework. I would also like to thank to Professor Tuncer B. Edil and Professor Peter J. Bosscher for serving on my thesis committee. Special thanks goes to Mr. Xiaodong Wang for his technical guidance in laboratory testing. The author is financially supported by the Turkish Ministry of Education during his study at the University of Wisconsin-Madison. This support is gratefully acknowledged. The findings and opinions expressed in this report are solely of the writer.

## TABLE OF CONTENTS

ABSTRACT .....	i
ACKNOWLEDGEMENT.....	ii
TABLE OF CONTENTS.....	iii
LIST OF FIGURES .....	ix
LIST OF TABLES .....	xv
1. INTRODUCTION.....	1
2. LITERATURE REVIEW.....	3
2.1 REVIEW OF EXISTING TEST DEVICES.....	3
2.1.1 Introduction .....	3
2.1.2 Large-Scale Direct Shear Box (ASTM D 5321) .....	3
2.1.3 Conventional Direct Shear Box (ASTM D 3080) .....	7
2.1.4 Ring Shear Device.....	8
2.1.5 Texas Double Interface Shear Device (TDISD) .....	9
2.2 TEMPERATURE EFFECTS ON GEOSYNTHETICS .....	11
2.2.1 Introduction .....	11
2.2.2 Cap and Liner Temperatures .....	11

2.2.3 Previous Interface Shear Strength Tests at Various Temperatures .....	12
2.3 TEMPERATURE EFFECTS ON POLYMERS .....	15
2.3.1 Glass Transition Temperature .....	15
2.3.2 Coefficient of Friction and Temperature .....	16
2.3.3 Temperature and Relaxation .....	16
3. MATERIALS AND METHODS .....	19
3.1 GEOSYNTHETICS .....	19
3.2 SHEAR TESTING .....	21
3.2.1 Texas Double Interface Shear Device .....	21
3.2.2 Constant Temperature Box .....	23
3.2.2.1 Actual Temperature Between the Specimens During Shearing .....	24
3.2.3 Temperature Influences on Pistons .....	24
3.2.4 Effect of the Textured Surface Area .....	25
3.2.5 Reproducibility .....	25
4. RESULTS AND ANALYSIS .....	28
4.1 INTRODUCTION .....	28

4.2 INTERFACE SHEAR STRENGTH VS. DISPLACEMENT RELATIONSHIP .....	28
4.3 FAILURE ENVELOPES .....	31
4.3.1 Linearity .....	31
4.3.2 Interface Shear Strength vs. Normal Stress .....	34
4.3.3 Interface Friction Angle vs. Temperature .....	34
4.3.4 Comparison With Other Data .....	36
4.4 RELAXATION AND ELONGATION .....	36
4.5 EFFECT OF SHEAR RATE AT VARIOUS TEMPERATURES .....	41
4.6 EFFECT OF MOISTURE .....	41
4.7 OBSERVATION AT HIGH TEMPERATURES ON THE SPECIMENS BEFORE SHEARING .....	44
5. SUMMARY AND CONCLUSIONS .....	45
6. REFERENCES .....	47
7. APPENDICES .....	50
APPENDIX A. NWNP GEOTEXTILE/TEXTURED GEOMEMBRANE AND NWNP GEOTEXTILE/SMOOTH GEOMEMBRANE ...	50
APPENDIX B. ERRORS DURING SHEARING .....	60
APPENDIX C. CALIBRATION OF LOAD CELLS AT VARIOUS TEMPERATURES .....	63

## LIST OF FIGURES

- Figure 2.1 (a) Direct Shear Box and (b) Ring Shear Device.
- Figure 2.2 Constant-Temperature Box (a) and Shear and Normal Forces (b).
- Figure 2.3 Soil Temperature from Corser et al. (1991).
- Figure 2.4 Soil Temperature from Khire et al. (1994).
- Figure 2.5 Relationship Between Temperature and Coefficient of Friction from Bely et al. (1982).
- Figure 3.1 Specimens: (a) NWNP Geotextile, (b) 2 mm Textured Geomembrane, and (c) 1.5 mm Smooth HDPE Geomembrane.
- Figure 3.2 Load Correction For Pistons.
- Figure 3.3 Piston Calibration: (a) left piston (b) right piston.
- Figure 3.4 Differences in Texturing for the Textured Geomembrane.
- Figure 4.1 Displacements of Peak and Residual Shear Strengths: (a) smooth HDPE geomembrane/NWNP geotextile, and (b) textured HDPE geomembrane/NWNP geotextile.
- Figure 4.2 Interface Shear Strength vs. Displacement: (a) Semilogarithmic Presentation, (b) Conventional graph.
- Figure 4.3 Orientation of Fibers at Peak Shear Stress (a) and at Residual Shear Stress (b).
- Figure 4.4 Effects of Temperature on Interface Strengths for Textured Geomembrane/NWNP Geotextile and Smooth HDPE Geomembrane/NWNP Geotextile: (A) Peak, (b) Residual.
- Figure 4.5 Effects of Temperature on Interface Friction Angle: (a) Textured Geomembrane/NWNP Geotextile, and (b) Smooth HDPE Geomembrane/NWNP Geotextile.
- Figure 4.6 Relaxation Time Factor at  $T=33^{\circ}\text{C}$ .

- Figure 4.7 Effect of Shear Displacement Rate on Interface Strength for Smooth HDPE Geomembrane/NWNP Geotextile at  $\sigma=21$  kPa at Different Temperatures: (a) Peak, (b) Residual.
- Figure 4.8 Effect of Shear Displacement Rate on Interface Strength for Textured Smooth HDPE Geomembrane/NWNP Geotextile at  $\sigma=21$  kPa at Different Temperatures: (a) Peak, (b) Residual.
- Figure A.1 Repeatable Interface Shear Strength Results at  $T=21^{\circ}\text{C}$ : (a) Peak and (b) Residual.
- Figure A.2 Interface Shear Strength vs. Displacement  $\sigma=7$  kPa at  $T=21^{\circ}\text{C}$ .
- Figure A.3 Interface Shear Strength Results Above  $\sigma=7$  kPa at  $T=21^{\circ}\text{C}$ .
- Figure A.4 Interface Shear Strength vs. Displacement Above  $\sigma=7$  kPa at  $T=21^{\circ}\text{C}$ .
- Figure A.5 Interface Shear Strength Results Above  $\sigma=7$  kPa at  $T=33^{\circ}\text{C}$ .
- Figure A.6 Interface Shear Strength vs. Displacement Above  $\sigma=7$  kPa at  $T=0^{\circ}\text{C}$ .
- Figure A.6 Interface Shear Strength Results Above  $\sigma=7$  kPa at  $T=21^{\circ}\text{C}$ .
- Figure A.7 Interface Shear Strength vs. Displacement Above  $\sigma=15$  kPa at  $T=33^{\circ}\text{C}$ .
- Figure A.8 Interface Shear Strength Results Above  $\sigma=7$  kPa at  $T=10^{\circ}\text{C}$ .
- Figure A.9 Interface Shear Strength Results Above  $\sigma=7$  kPa at  $T=0^{\circ}\text{C}$ .
- Figure B.1 When Aluminum Plates Of The TDISD Were Not Maintained Parallel To Each Other: NWNP Geotextile/Smooth HDPE.
- Figure C.1 Load Cell Calibration at Various Temperatures.
- Figure C.2 Load Cell Calibration at Various Temperatures.
- Figure C.3 Load Cell Calibration at Various Temperatures.
- Figure C.4 Load Cell Calibration at Various Temperatures.

## LIST OF TABLES

- Table 2.1 Advantages and Disadvantages of Test Devices for Measuring Interface Shear Strength.
- Table 3.1 Mass Per Unit Area and the Thickness of the Specimens.
- Table 4.1 Friction Angles for NWNP Geotextile/Smooth HDPE Geomembrane.
- Table 4.2 Friction Angles for NWNP Geotextile/Textured HDPE Geomembrane.
- Table 4.3  $\tan\phi$  for NWNP Geotextile/Smooth HDPE Geomembrane Interface.
- Table 4.4  $\tan\phi$  for NWNP Geotextile/Textured HDPE Geomembrane Interface.
- Table 4.5 NWNP Geotextile/Smooth HDPE Geomembrane Interface Shear Friction Angles at Room Temperature (21°C).
- Table 4.6 NWNP Geotextile/Smooth HDPE Geomembrane Interface Shear Friction Angles at Room Temperature (21°C).

## SECTION ONE

### INTRODUCTION

The capacity of landfill is determined by its volume (area, height, and side slopes). The area and height are usually determined by property limits and regulations, but the side slope angle is based on engineering judgment and operational performance. The side slope of the landfill are often made as steep as possible. However, when the slope is too steep, the protective soil cover and geosynthetic liners can become unstable. This movement will result in an increase in maintenance costs and can destroy a containment facility. Designs must balance the need for capacity against the risk of the failure.

In the United States, containment facilities for municipal and toxic waste often have cover systems containing a variety geosynthetic materials. NWNP geotextiles and HDPE geomembranes are the most common geosynthetics. The use of geosynthetics can lead to stability problems. For example, the slope failure at the Kettleman Hills facility in Kettleman City, California in 1988 was due to the smooth surface (and hence, the low interface shear strength) of a HDPE geomembrane (Byrne et al. 1992, Gilbert et al. 1995).

Seasonal temperature changes may affect the interfacial properties of geosynthetics and hence slope stability. The focus of this study was to assess how temperature affects interface strengths between geotextiles and geomembranes.

This objective was met by conducting shear tests at various temperatures using the Texas Double-Interface Shear Device.

## SECTION TWO

### LITERATURE REVIEW

#### 2.1 REVIEW OF EXISTING TEST DEVICES

##### 2.1.1 Introduction

Large-scale direct shear boxes, traditional direct shear boxes, and ring shear devices are the most generally used devices for measuring interface shear strength. The common disadvantage of these devices is frictional resistance and eccentric loading. The basic design of the Texas double interface shear device (TDISD) minimizes these effects (Gilbert et al. 1995). The advantages and disadvantages of each test device for measuring interface shear strength is summarized in Table 2.1. Figs. 2.1 and 2.2 illustrate various devices.

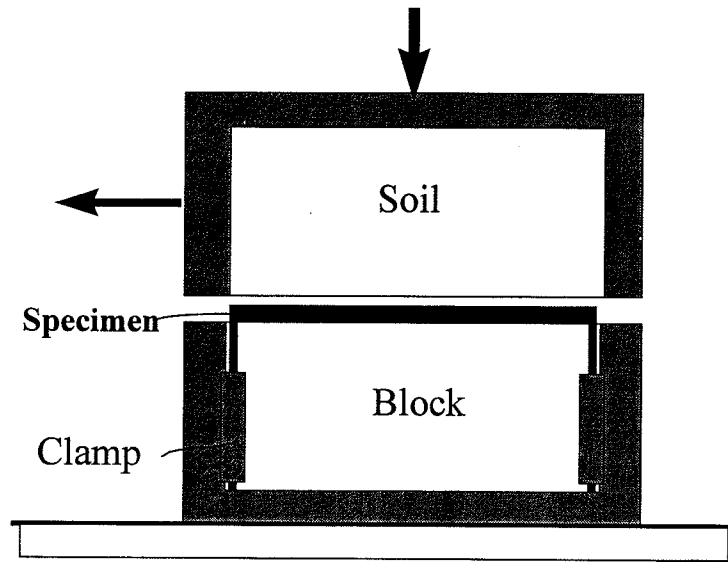
##### 2.1.2 Large-Scale Direct Shear Box (ASTM D 5321)

The large-scale direct shear box is the most common device used for measuring interface strength (Stark et al. 1994, Gilbert et al. 1995). This device consists of a stationary and traveling container (Fig. 2.1). The containers are either square or rectangular, with dimensions of at least 300 mm wide by 300 mm long. The specimen is placed between the two containers. A vertical normal load is applied, and the interface is sheared at a constant rate of displacement.

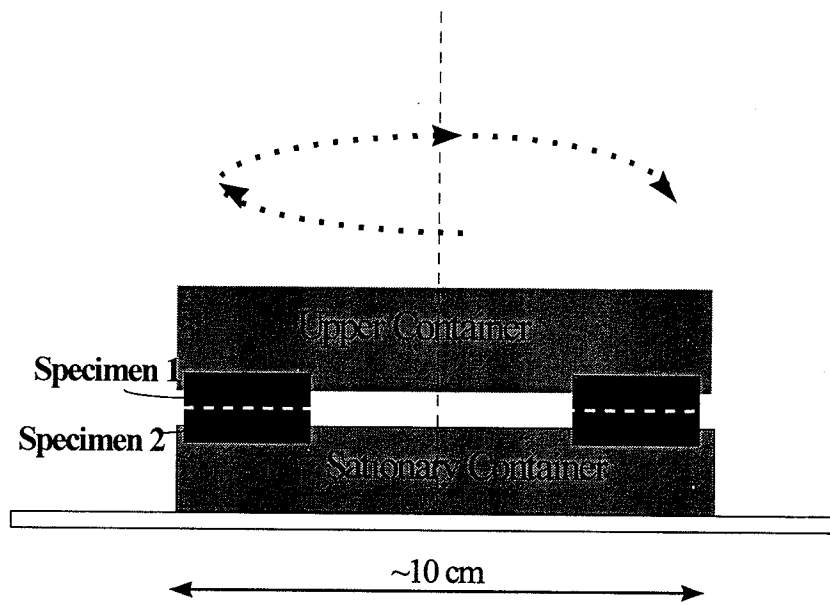
The advantages of this method are that it is widely used in the industry, has an standard procedure (ASTM D 5321), can be scaled larger than the conventional

Table 2.1 Advantages and Disadvantages of Test Devices for Measuring Interface Shear Strength

DEVICES	ADVANTAGES	DISADVANTAGES
Large-Scale Direct Shear Box	Industry Standard Large Scale Large Displacements	Machine Friction Load Eccentricity Limited Continuous Displacements Expensive
Conventional Direct Shear Box	Experience with Soil Inexpensive	Machine Friction Load Eccentricity Small Scale Limited Displacements
Ring Shear Device	Unlimited Continuous Displacement	Machine Friction Anisotropic Shearing Small Scale
Texas Double Interface Shear Device	Simple Minimal Machine Friction Large Displacements Inexpensive Minimal Load Eccentricity	Limited Continuous Displacements Friction Problems in the Pistons



(a)



(b)

Figure 2.1 (a) Direct Shear Box and (b) Ring Shear Device.

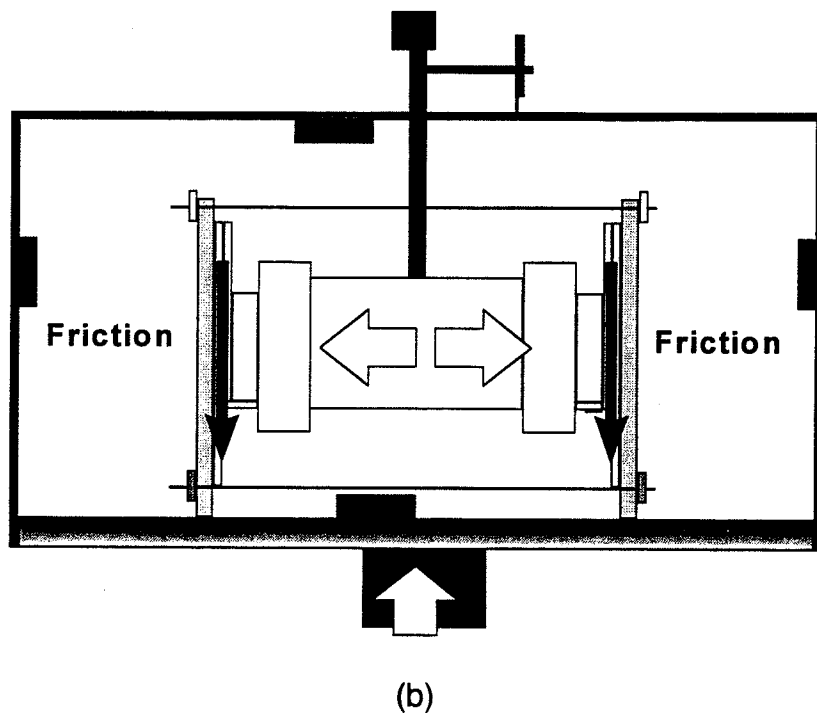
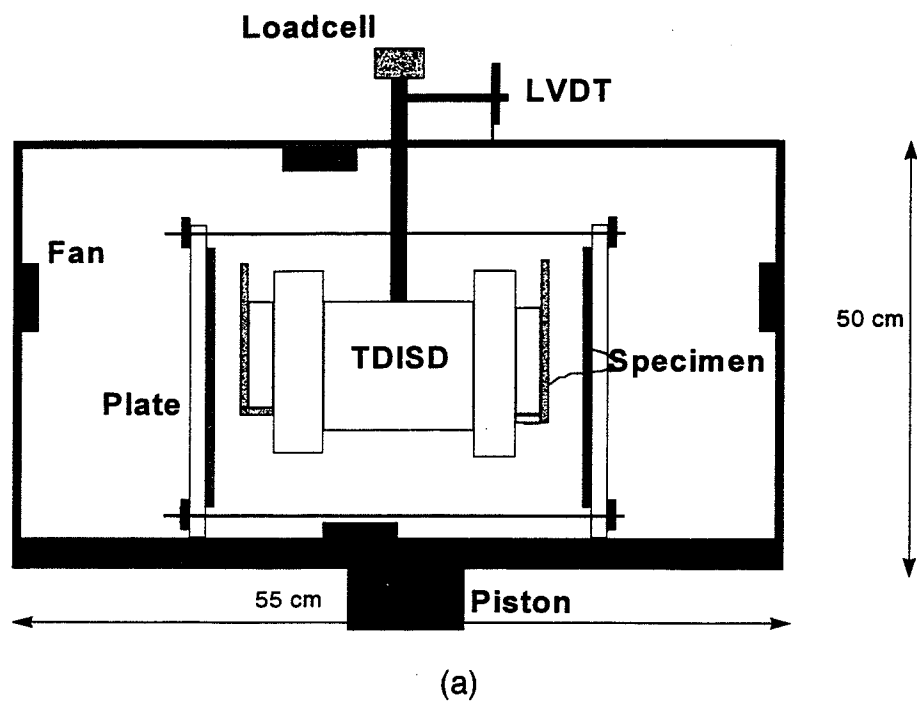


Fig. 2.2. Constant-Temperature Box (a) and Shear and Normal Forces (b)

direct shear box or the ring shear box, a large sample size can be used, and boundary effects are minimized.

The disadvantages of the method are machine friction, eccentric shear loading, limited continuous displacements, and high cost. Because the traveling container is subjected to the same normal load as the interface, machine friction develops between the container and the rest of the apparatus. The normal load is placed on bearings to minimize friction. These bearings do not eliminate the machine friction completely, and they are expensive and may limit the applied normal load. Machine friction can be minimized by applying low normal stresses. Load eccentricity occurs when the test interface contracts or dilates relative to line application of the shear force. The force then becomes eccentric and the normal stresses on the interface will be non-uniform. As a result eccentricity of the loading will affect the interface shear results.

### **2.1.3 Conventional Direct Shear Box (ASTM D 3080)**

The conventional direct shear box is similar to the large-scale direct shear box, but smaller in scale (Fig. 2.1). The dimensions of the device can be as small as 7 cm x 7 cm (Gilbert et al.1995). A conventional direct shear test is less expensive than one employing the large-scale direct shear box, is widely used in the industry, and has a standard procedure (ASTM D 3080). Conventional direct shear tests provide reasonable peak interface shear strengths (Stark et al. 1994).

But this method shares some of the problems of the large-scale direct shear box. Machine friction, load eccentricity, boundary effects, small scale, and limited displacements are disadvantages of this method. Usually the displacements are less than 10 mm, for the specimens are usually only 10 cm x 10 cm. Like the former method, machine friction can be minimized by applying low normal stresses.

#### **2.1.4 Ring Shear Device**

This new shear device (Fig. 2.1) has recently been used for measuring interface strengths for geosynthetics (Stark et al. 1994). The traveling container is rotated at a constant rate relative to the stationary container. The sample is in the shape of a ring. Like the devices described above, the samples are attached between the two containers.

The most significant advantages of the ring shear device are unlimited continuous-shear displacement and a constant cross-sectional area during shearing. But the disadvantages of this device include non-uniform displacements in the radial direction, machine friction, small sample size (no larger than 10 cm in diameter) and its operating cost. The small specimen size, especially for anisotropic materials or materials with large asperities, limits the usefulness of this device. Finally, rotational shearing may not represent true field deformation conditions (Stark et al. 1994).

### **2.1.5 Texas Double Interface Shear Device (TDISD)**

The Texas double interface shear device (TDISD) can be used as an alternative test method (Figure 2.2). The device consists of two pistons and two rectangular plates. Rectangular or square geosynthetic specimens are located between the pistons and the plates. No resistance to shear is contributed by the device itself.

The Texas double interface shear device minimizes both machine friction and load eccentricity. It is easy to use and inexpensive, with none of the limitations associated with either large sample sizes or high normal stresses. Bearings are not required, and the device can be constructed to fit into conventional triaxial load presses. Deformations due to dilation or contraction at the interface during shear are balanced and eccentric loading is eliminated.

The disadvantages of the TDISD are that it is unable to accommodate unlimited continuous displacement, and currently there is no standard procedure. However, large relative displacements are possible if the stationary containers are longer than the traveling container (Gilbert et al. 1995). Friction problems in the piston can impair this device, particularly when the applied normal stress is low (<15 kPa). Maintaining a constant distance between the aluminum plates is another concern; when the plates are not parallel, anomalous results are obtained.

## **2.2 TEMPERATURE EFFECTS ON GEOSYNTHETICS**

### **2.2.1 Introduction**

Temperature has a significant effect on the mechanical properties of polymers, such as modulus, tensile strength, and hardness. Polymers soften and eventually flow as they are heated. Therefore, it is important to know the limiting temperatures at which polymer components can still be loaded with moderate deformations. Given the importance of temperature, it is surprising that there has been only limited studies of the behavior of geosynthetic interfaces as a function of temperature.

### **2.2.2 Cap and Liner Temperatures**

Corser et al. (1991) investigated temperature profiles for three cover sections (Fig. 2.3). They indicate that overlying vegetative soil cover acts both to insulate the clay and geomembrane and to reduce the daily change in temperature between sunrise and sunset. The temperatures at the clay surface varied between 15°C and 30°C. The temperature profiles for the cover section with the HDPE exposed at its surface and no overlying vegetative cover indicate that the clay surface experiences large temperature fluctuations on a daily basis. Temperatures in the clay were as high as 43°C. Similar or more extreme geomembrane temperatures can be expected.

Montgomery et al. (1990) collected data on soil temperatures of for three final cover designs at the Omega Hills Landfill, located near Milwaukee, Wisconsin. Soil temperature probes indicated substantial moderation of temperature fluctuations in the soil cover relative to air temperature. At a depth of 30cm below the cover surface, soil temperatures ranged from approximately 27°C during August to 7°C during the winter months. The longest period of freezing at 30 cm depth was approximately 8 weeks.

Khire et al. (1994) collected temperature data from final cover test sections. Soil temperatures showed a sinusoidal trend (Fig. 2.4). The temperatures fluctuated over a greater range near the surface, and became more stable with depth. At a depth of 15 cm below the cover surface, soil temperatures ranged from approximately 1°C in January to 33 °C during August.

Similar temperature fluctuations should be expected in the geosynthetic layers used in caps. Moreover, exposed geosynthetics may undergo larger temperature fluctuations. For example, geomembranes can become as much as 50°C higher than air temperature because of their black color.

### **2.2.3 Previous Interface Shear Strength Tests at Various Temperatures**

Pasqualini et al. (1993) showe that temperature affected the interface shear strength between three different smooth LDPE geomembranes and a NWNP geotextile. Temperatures used in the experiments varied from 25°C to 30°C between geosynthetics. When the temperature was increased from 26°C to 30°C,

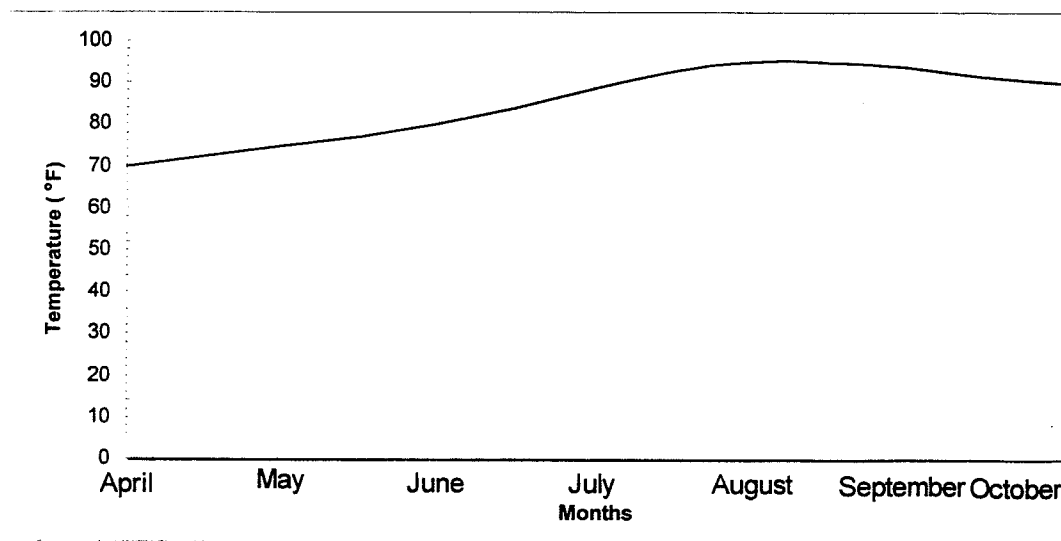


Figure 2.3. Soil Temperature (from Corser et al. 1991).

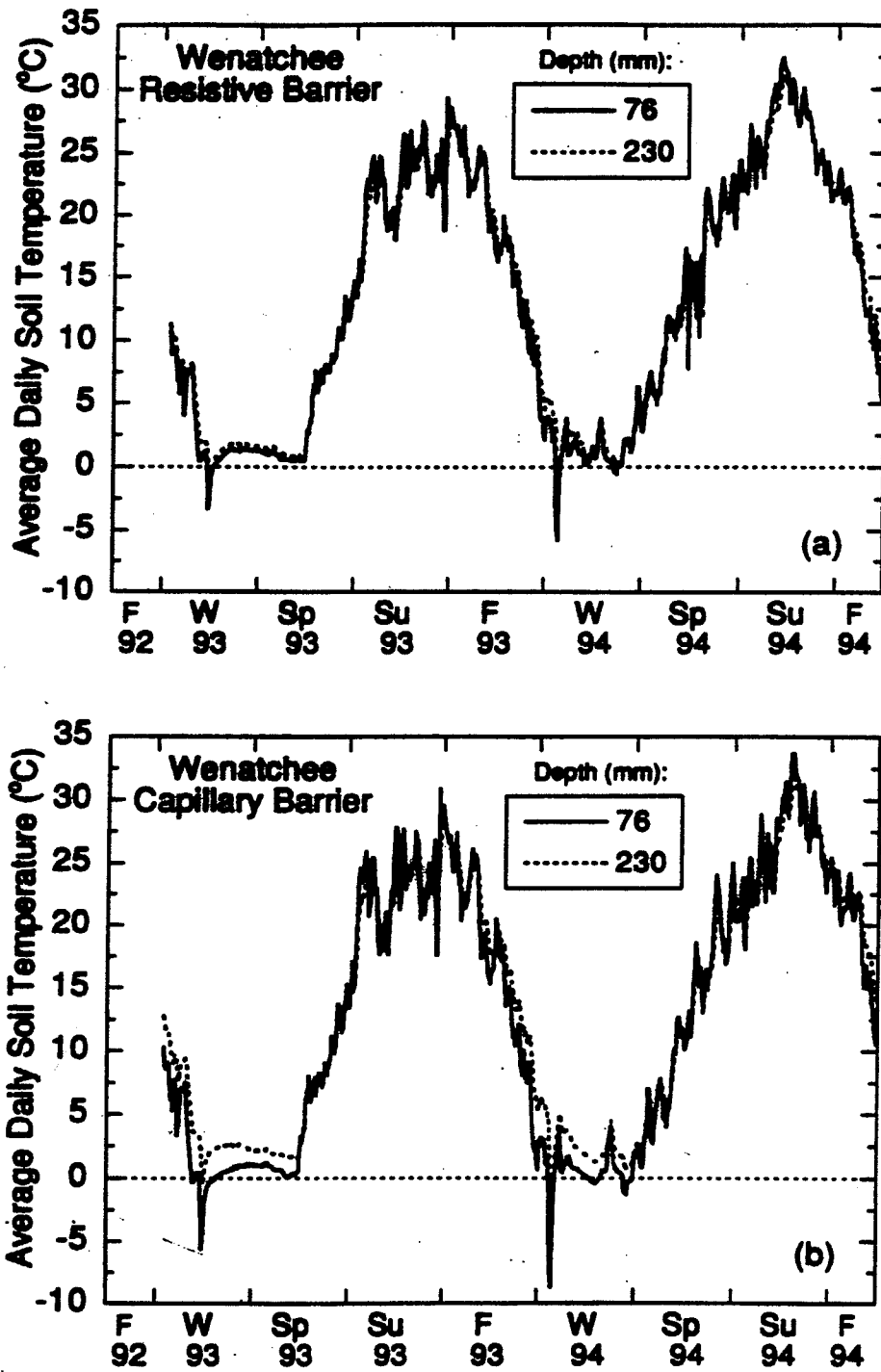


Figure 2.4. Soil Temperatures (from Khire et al. 1994).

the interface shear strength increased 16%-33%. Pasqualini et al. also stressed the importance of accounting for temperature when experimental data from different laboratories are compared. They also found that the tests carried out in a wet condition gave shear resistance that was systematically 10% lower than those obtained in the dry condition.

## **2.3 TEMPERATURE EFFECTS ON POLYMERS**

### **2.3.1 Glass Transition Temperature**

As a polymer, such as HDPE or PP, goes from the glassy state to the rubber state, or vice versa, it is said to pass through the glass transition temperature ( $T_g$ ). The glass transition temperature corresponds to a mobility change in a polymer. Transition temperatures for HDPE and polypropylene are  $-110^{\circ}\text{C}$  and  $-27^{\circ}\text{C}$  respectively (Daniels et al. 1989). In glassy state thermal energy is not sufficient to permit polymer chains to move relative to another. The rubber state has a temperature range above that of the glassy state and is characterized by greater mobility.

For amorphous polymers such as HDPE and PP, at  $T_g$  or higher, polymer molecules are active enough to relieve stress concentrations (Nielsen et al. 1994). Likewise, when the temperature increases, concentrated shear stresses are relieved, and more shear stress is required to overcome friction between geosynthetics.

### **2.3.2 Coefficient of Friction and Temperature**

An increase in the internal temperature of a polymer, or an increase in the temperature of the testing conditions will result in an increase in the coefficient of friction between polymers (Daniels et al. 1989). The variation in the coefficient of friction with temperature is directly related to the chemical composition of the polymer, as well as its intermolecular interaction. The coefficient of friction of polyethylene increases slightly as its temperature increases (Bely et al. 1982). The relationship between coefficient of friction and temperature is shown in Fig. 2.5. The coefficient of friction for PET begins to increase due to a rise in the activity of molecular interaction at the polymer surface (Bely et al. 1982).

### **2.3.3 Temperature and Relaxation**

Stress relaxation is time and temperature dependent, especially at glass transition temperatures. The time it takes for applied stresses to relax within a material is called the relaxation time. Relaxation time decreases exponentially with increasing temperature (Osswald et al. 1995). Relaxation time can be from few seconds to a few days, depending on the polymer.

In general, polymers have long relaxation times. For example, tensile test or shear test is normally completed before the polymer will have relaxed. The relaxation time is long for all polymers at low temperature (Daniels et al. 1989).

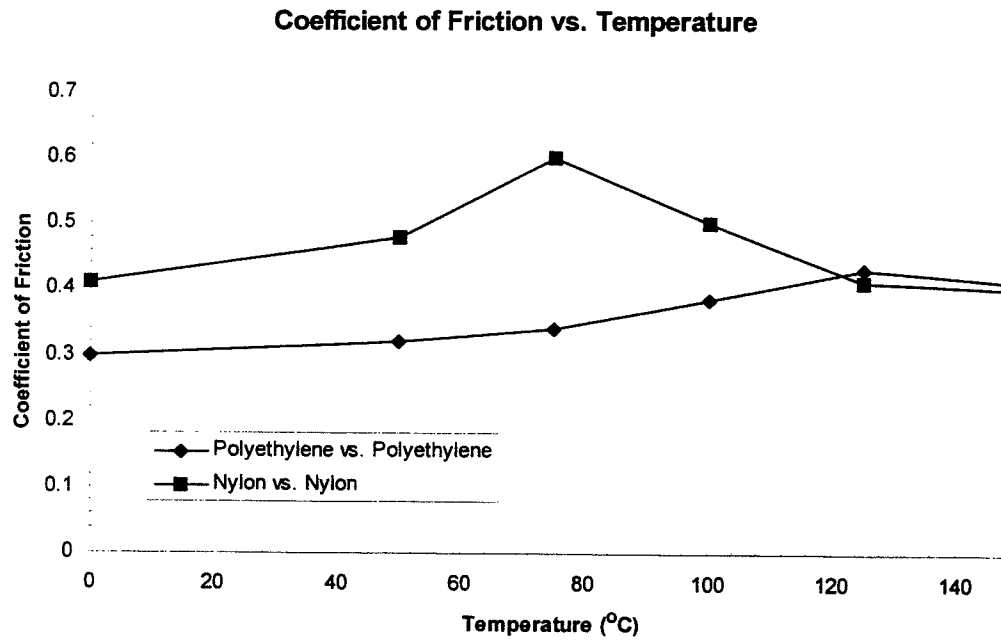


Figure 2.5 Relationship Between Temperature and Coefficient of Friction (from bely at al. 1982).

Fibers in polypropylene geotextiles lose their tensile strength due to thermal induced relaxation Tisinger et al. (1991).

## SECTION THREE

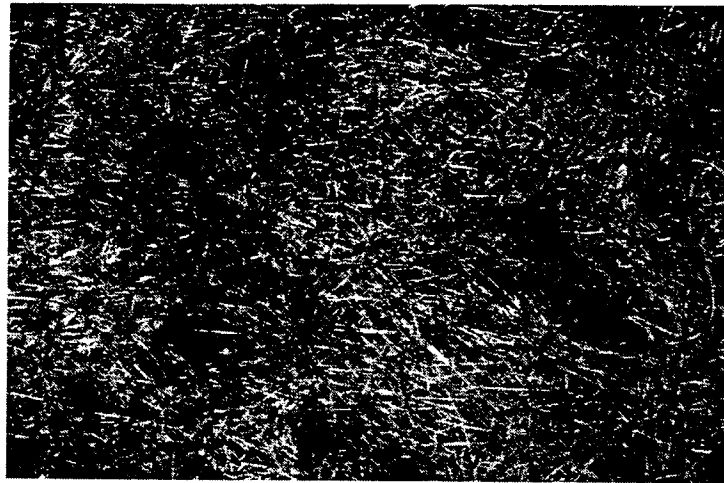
### MATERIALS AND METHODS

#### 3.1 GEOSYNTHETICS

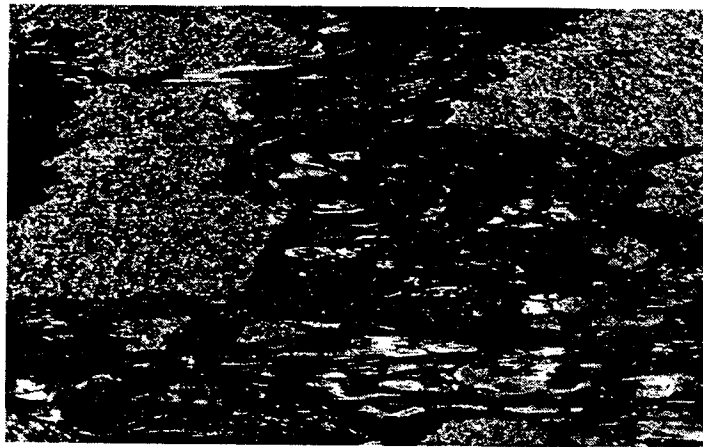
A non-woven needle punched (NWNP) geotextile and two high density polyethylene (HDPE) geomembranes were used. The NWNP geotextile was made of polypropylene fibers and was manufactured by Hoechst-Celanese, Inc. The smooth HDPE and impingement textured HDPE geomembranes were manufactured by National Seal Company. All the specimens were 30 cm long and 18 cm wide. Other characteristics are given in Table 3.1. Figure 3.1 shows images of the surface of each geosynthetic.

Table 3.1. Mass Per Unit Area and the Thickness of the Specimens

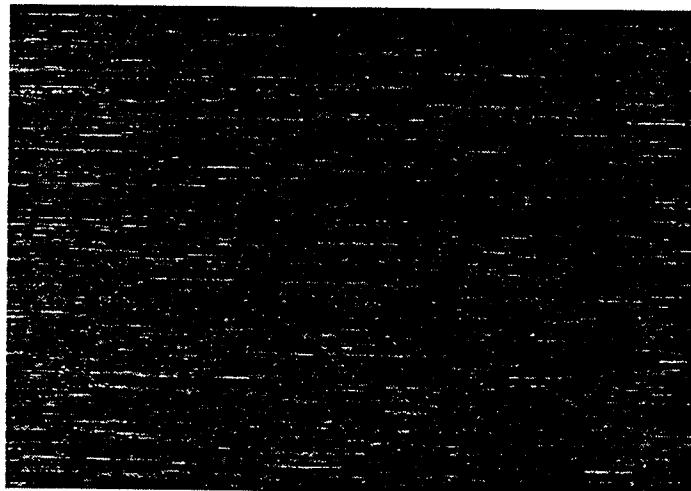
Specimen	HDPE Smooth Geomembrane	HDPE Textured Geomembrane	NWNP Geotextile
Mass Per Unit Area (ASTM D 5261)	1441 g/m <sup>2</sup>	1617 g/m <sup>2</sup>	270 g/m <sup>2</sup>
Thickness (ASTM D 5199)	1.5 mm	2 mm	5 mm



(a)



(b)



(c)

Figure 3.1 Specimens: (a) NWNP Geotextile, (b) 2 mm Textured Geomembrane, and (c) 1.5 mm Smooth HDPE Geomembrane.

## 3.2 SHEAR TESTING

### 3.2.1 Texas Double Interface Shear Device

A TDISD was used for testing. The outer stationary frames consist of aluminum plates connected by six rods, each with a diameter of 25 mm. The outer plates are 25 mm thick, 152 mm wide, and 305 mm long. The inner loading apparatus consists of two aluminum plates attached to a double-ended air piston. The inner plates are 25 mm thick, 102 mm wide, and 102 mm long. Normal force is applied to the interfaces by applying air pressure to the piston. The geosynthetics are clamped to the inner and outer plates using metal strips and bolts (Fig. 2.2).

The TDISD device fits into a standard loading press used for triaxial shear testing. The outer plates rest on the base pedestal of the press, and the inner section is connected to the loading piston. The base pedestal is raised at a constant rate of displacement. Shear displacement is measured with a LVDT, and the shear force is measured with a load cell. The shear force is corrected to account for the weight of the inner apparatus, including the piston. The normal force can be estimated from the pressure in the piston; however, the normal force applied to the interface is slightly smaller than the piston pressure because of friction within the piston.

To measure the efficiency of the piston, two load cell cells were located between the pistons and the aluminum plates. Both pistons were found to apply a stress equal to 95% of the applied air pressure (Fig. 3.2).

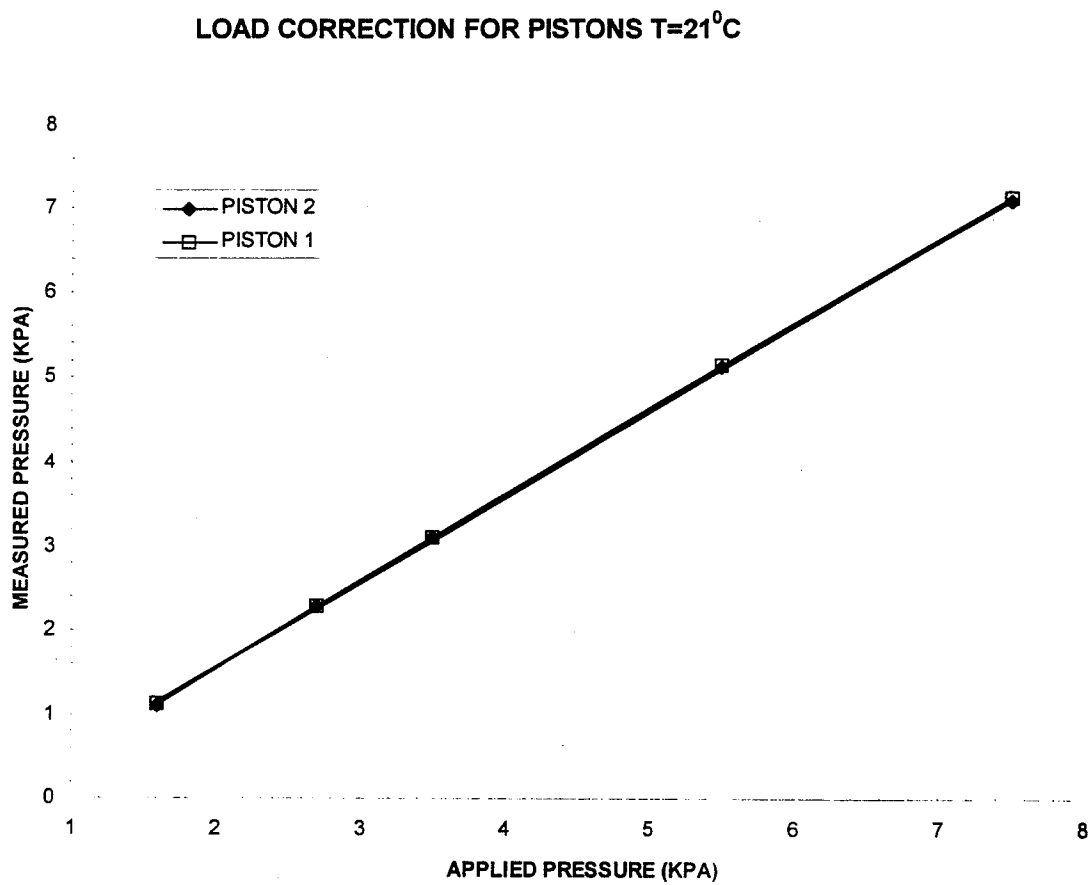


Figure 3.2. Load Correction For Pistons.

A loading frame with a capacity of 10,000 kg and a maximum strain rate of 2.5 cm/min was used. Strain rates used in the tests were 0.15 cm/min, 0.09 cm/min, and 0.11 cm/min.

### **3.2.2 Constant Temperature Box**

A constant temperature box was designed to provide constant temperature conditions during testing. The box was 50 cm tall, 55 cm long, and 26 cm wide. The base of the box was made of steel. Other parts were made of 0.5 cm clear acrylic. Four fans circulate air within the box to ensure uniform temperature.

An LVDT was located on top of the box that had a capability of measuring vertical displacements up to 10 cm. The LVDT was located outside the box so that it would not be affected by temperature changes.

The box was maintained at elevated temperatures using four lamps and a temperature controller with a thermocouple. When the desired temperature was reached, the controller shut off the lamps; when the temperature decreased, the controller turned on the lamps. Temperatures were set at 0°C, 10°C, 21°C, 33°C using the controller.

Cooler temperatures were obtained by circulating cool air through the box with two tubes. One tube removed cold air from a refrigerator and blew the air into the box. The other tube evacuated air from inside the box and returned it to the refrigerator. A minimum temperature of 0°C was obtained using this method.

The normal stress was applied and shearing was initiated immediately after thermal equilibrium was obtained. Two thermometers were located between the specimens (on either side of the piston) to check the temperature. To reach the expected temperatures quickly, the acrylic was covered with aluminum foil. For example, heating to 33°C required 40 min. without foil, whereas only 10 min. was required with foil.

### **3.2.2.1 Actual Temperature Between the Specimens During Shearing**

Friction will generate heat on the interface surface as it is sheared. Heat is more easily dissipated by polymers than other materials, so it tends to have a greater effect in their properties. When a polymer is stressed, some of the energy put into the polymer is stored in elastic and plastic deformations and some of its converted to heat (Daniels et al. 1989; Bely et al. 1982). Thus, during shearing the actual temperature between the contacted surfaces of the specimens could be higher than the box temperature. Nevertheless, because the rate of shear was low and air was constantly circulated through the box, it is unlikely that the interface temperature differed significantly from the box temperature.

### **3.2.3 Temperature Influences on Pistons**

Temperature effects on friction in the pistons were measured by increasing the temperature from 0°C to 50°C and applying different piston loads. The effect of temperature on the load cells were ignored (Fig. 3.3). Results of the tests showed

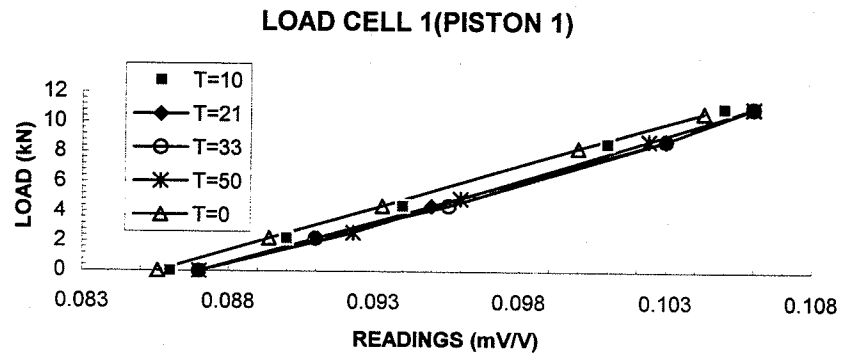
that temperatures does not affect the piston force. Also, there were no changes in the volume of the pistons. Fig. 3.2 shows the relationship between the applied pressure and measured normal stress at room temperature. Similar results were obtained at temperatures of 0°C, 10°C, and 33°C.

### **3.2.4 Effect of the Textured Surface Area**

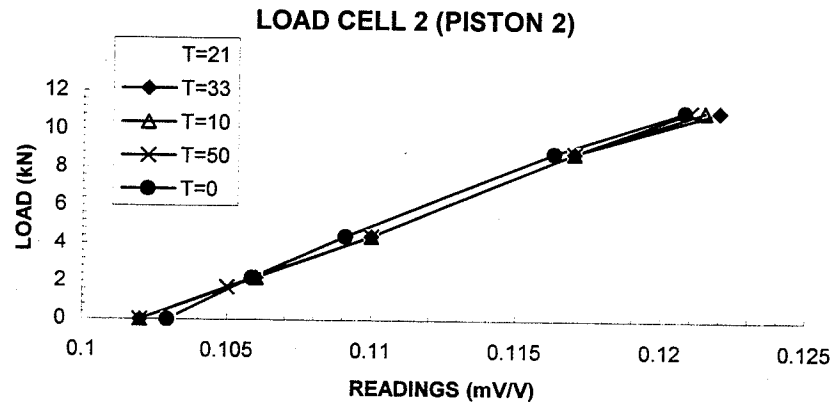
In some cases, under the same normal stress and temperature, slightly different interface shear strengths were obtained between textured geomembrane and a NWNP geotextile. For example, when two shear tests were conducted with 49 kPa normal stress at 10°C, the interface shear test conducted with a geomembrane with more textured surface area gave 0.9 kPa more shear strength. This suggested that the textured surface area can affect the interface shear results at various temperatures even though it is from the same product (Fig. 3.4).

### **3.2.5 Reproducibility**

The interface shear tests were conducted at least two times under same conditions (same temperature, same normal stress) to verify the reproducibility of the TDISD. Repeatable results were obtained. The coefficient of variation was typically small, being between 0.05 to 0.1.

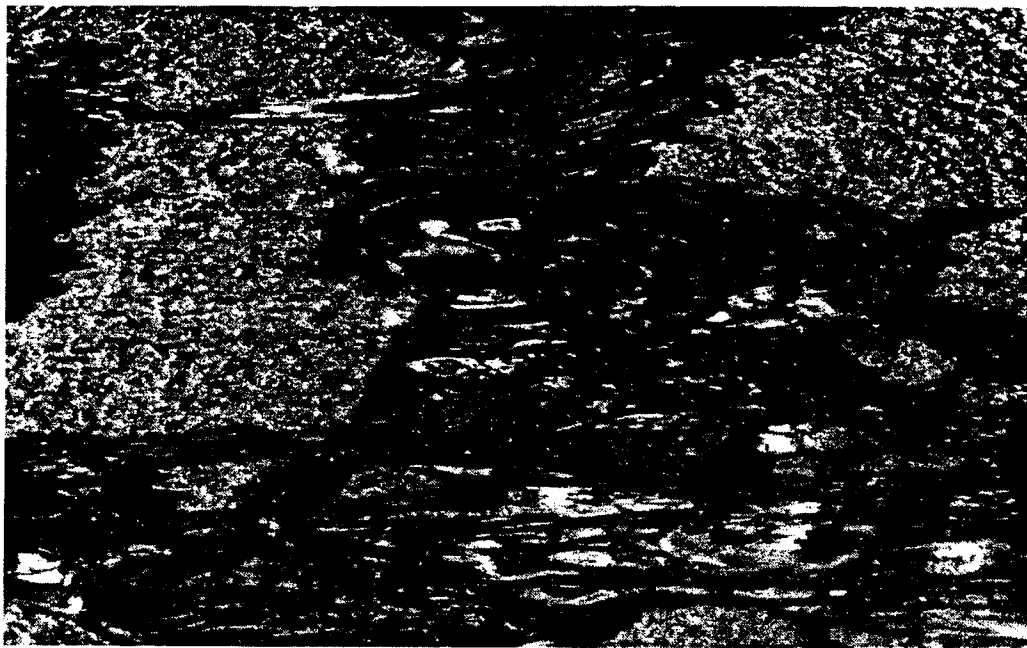


(a)



(b)

Figure 3.3 Piston Calibration (a) left piston (b) right piston.



(a)



(b)

Figure 3.4. Differences in Texturing for the Textured Geomembrane.

## SECTION FOUR

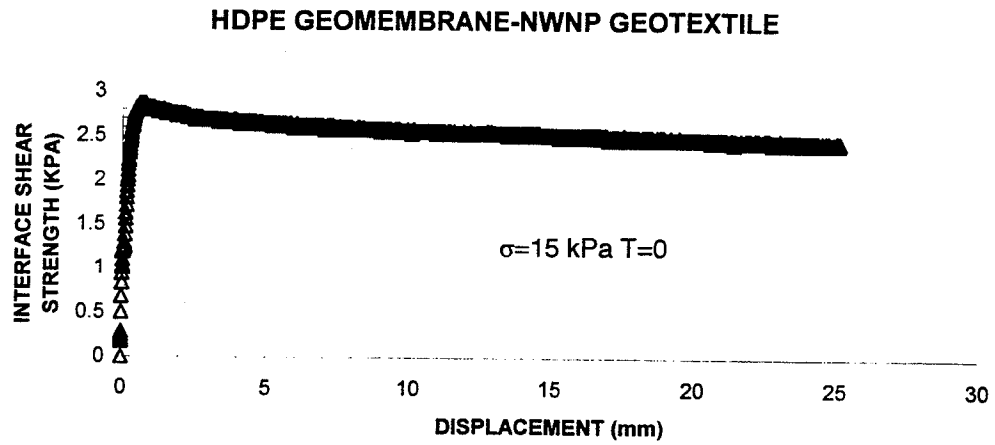
### RESULTS AND ANALYSIS

#### 4.1 INTRODUCTION

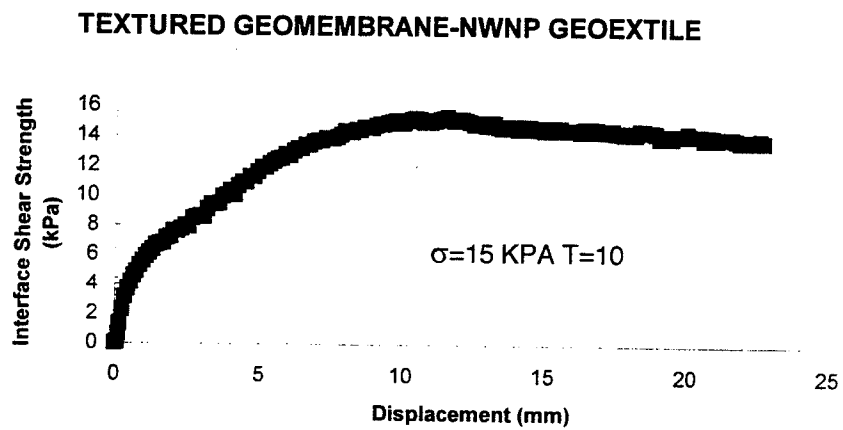
Approximately 100 interface shear tests were conducted on smooth HDPE geomembrane/NWNP geotextile and textured geomembrane/NWNP geotextile interfaces at temperatures of 0°C, 10°C, 21°C, and 33°C. Results of the tests are described in the following sections.

#### 4.2 INTERFACE SHEAR STRENGTH vs. DISPLACEMENT RELATIONSHIP

Peak interface strengths for the smooth HDPE/NWNP geotextile was mobilized at relatively small displacements ( $\delta$ ) between 1 and 2 mm (Fig 4.1). Larger displacements (10-15 mm) were required for the textured HDPE/NWNP geotextile interface. Figure 4.1 shows that the residual interface strengths were reached at displacements between 15 and 20 mm for the smooth HDPE/NWNP geotextile interface and between 20 and 25 mm for the textured HDPE/NWNP geotextile interface. The residual shear strength was defined as the shear strength at 25 mm displacement. Figure 4.2 presents a semi-logarithmic representation of interface shear strength vs. displacement graph, and shows that fully residual conditions were not achieved during the tests. However the residual strengths were reported are likely to be very similar, at best slightly higher, than fully residual strengths.



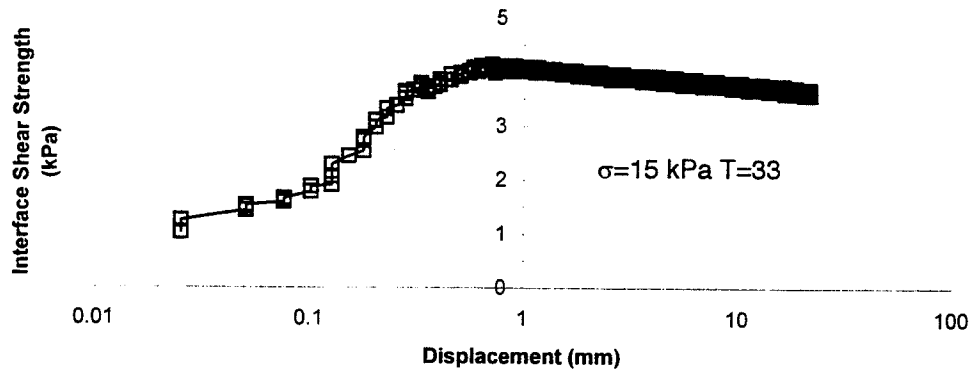
(a)



(b)

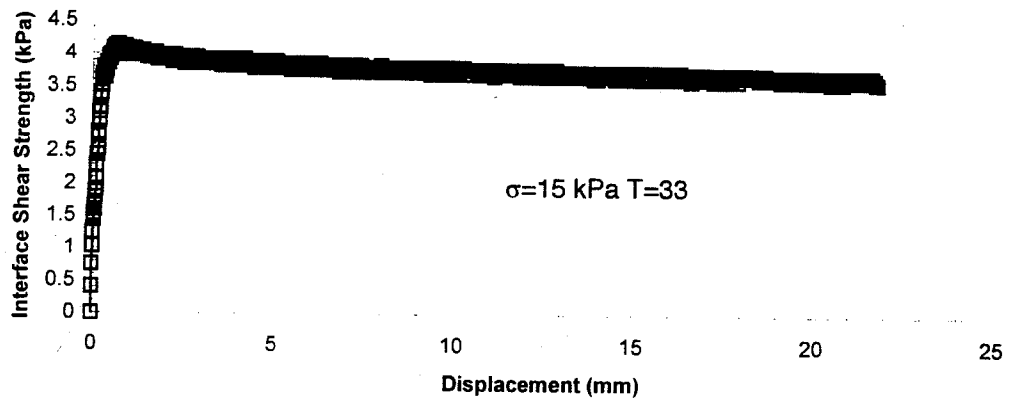
Figure 4.1 Displacements of Peak and Residual Shear Strengths: (a) smooth HDPE geomembrane/NWNP geotextile, and (b) textured HDPE geomembrane/NWNP geotextile.

HDPE GEOMEMBRANE-NWNP GEOEXTILE



(a)

HDPE GEOMEMBRANE-NWNP GEOEXTILE



(b)

Figure 4.2 Interface Shear Strength vs. Displacement: (a) semilogarithmic presentation, (b) conventional graph.

The post-peak strength loss exhibited by the textured geomembrane/non-woven geotextile was caused by pulling out and/or tearing the filaments from the geotextile during shear. Additional shear displacement appeared to comb or orient these detached fibers parallel to the direction of shear. Figure 4.3 presents an image of a NWNP geotextile prior to shearing with textured geomembrane. Polishing of the textured surface of the geomembrane may have also contributed to the post-peak strength loss, especially under high normal stress ( $>49$  kPa). Similar results have been presented by Stark et al. (1996). The post-peak strength loss exhibited by the smooth geomembrane/non-woven geotextile was due to the orientation of the fibers (fibers become parallel to the direction of shear). For smooth HDPE geomembrane/NWNP geotextile and for textured geomembrane/NWNP geotextile, the residual interface strength at various temperatures were 7 to 18 percent and 1 to 1.5 percent, respectively, lower than the peak values.

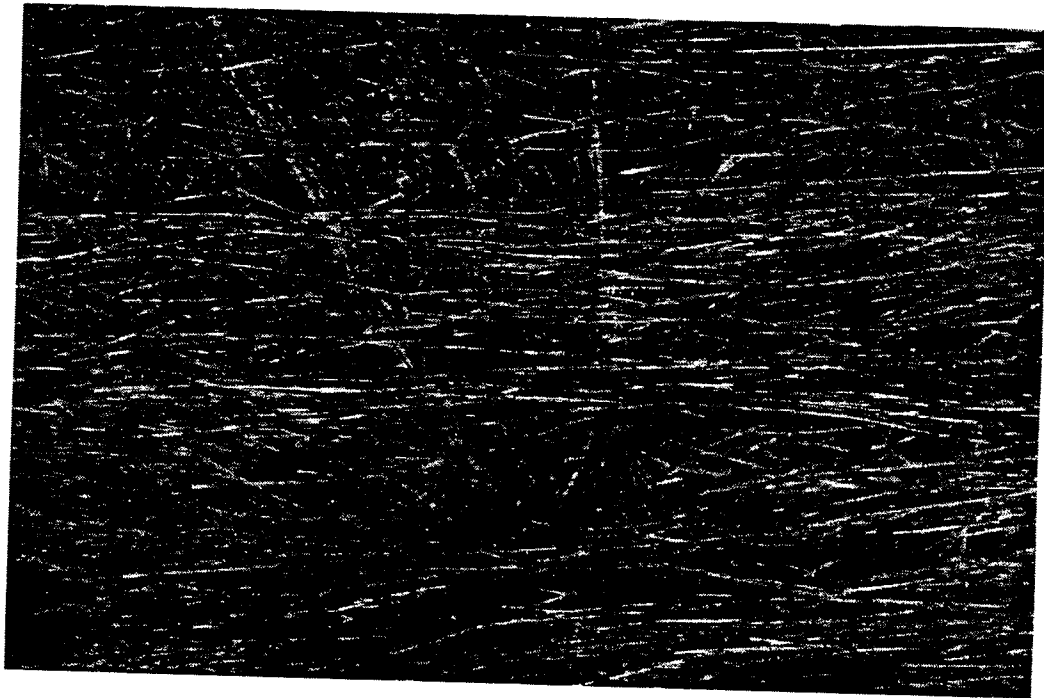
### **4.3 FAILURE ENVELOPES**

#### **4.3.1 Linearity**

Figure 4.4 presents the peak and residual failure envelopes for the smooth HDPE geomembrane/NWNP geotextile and textured geomembrane/NWNP geotextile interfaces. The failure envelopes are approximately linear within the stress ranges tested. As a result, peak and residual failure envelopes can be represented by friction angles (Bove et al. 1990).



(a)



(b)

Figure 4.3 Orientation of Fibers at Peak Shear Stress (a) and at Residual Shear stress (b).

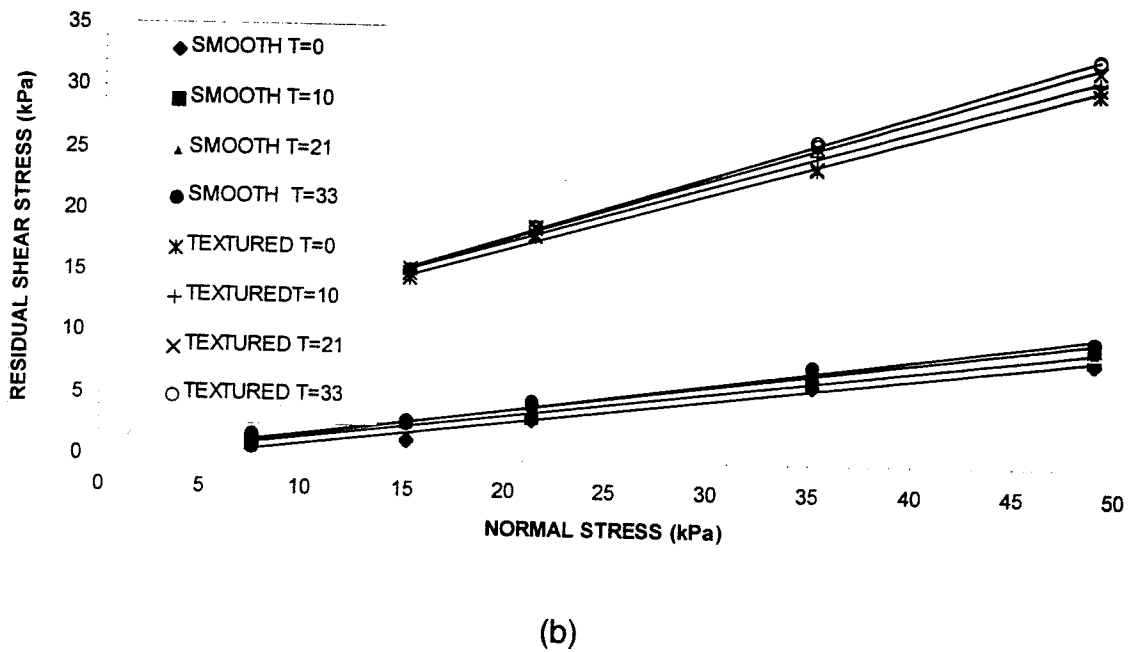
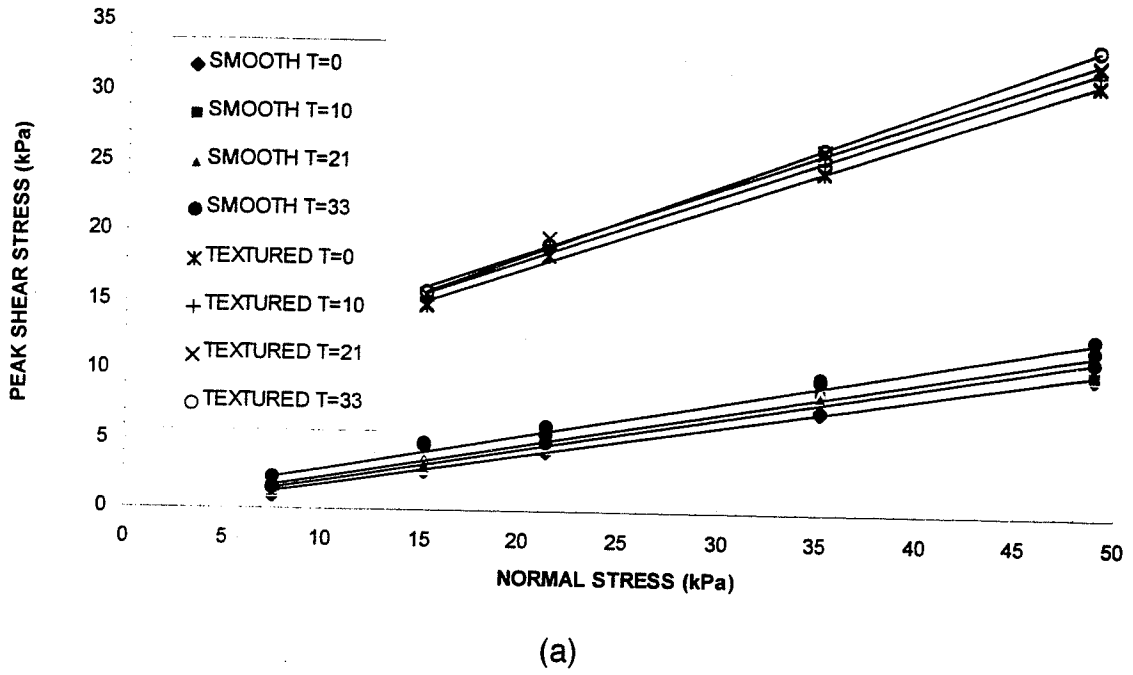


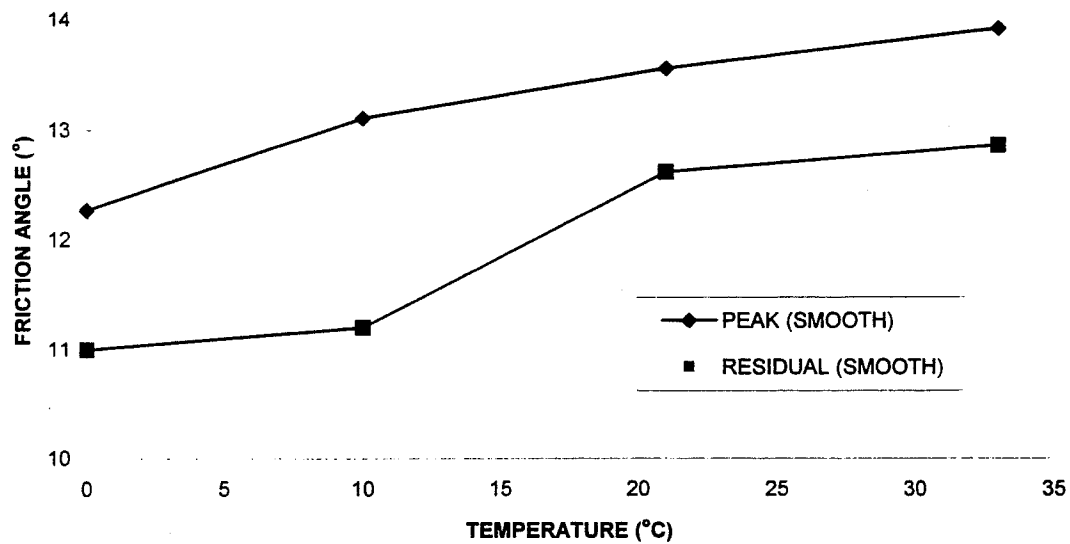
Figure 4.4 Effects of temperature on interface strengths for textured geomembrane/NWNP geotextile and smooth HDPE geomembrane/NWNP Geotextile: (a) peak, (b) residual.

#### **4.3.2 Interface Shear Strength vs. Normal Stress**

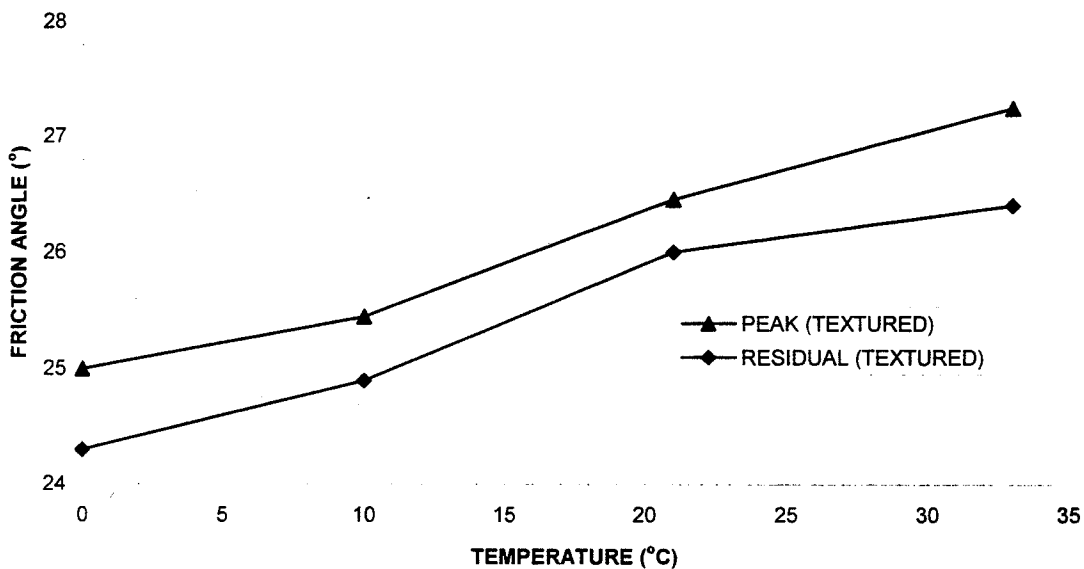
The test results show that the interface shear strength increases with increasing temperature. When the temperatures were increased from 0°C to 33°C at normal stress of 49 kPa, the peak interface shear strength increased 8.3% and 20% for textured gemembrane/NWNP geotextile and for smooth gemembrane/NWNP geotextile, respectively. The residual strengths increased 6.4% and 19.3% for textured gemembrane/NWNP geotextile and for smooth gemembrane/NWNP geotextile, respectively. The percentage increase in interface shear strengths at low normal stress was different. For example, when the temperature was increased from 0°C to 33°C at normal stress of 15 kPa, the peak interface shear strength increased 6 % and 68 % for textured gemembrane/NWNP geotextile and for smooth gemembrane/NWNP geotextile respectively. The residual strengths increased 5.2% and 94% for textured gemembrane/NWNP geotextile and for smooth gemembrane/NWNP geotextile, respectively.

#### **4.3.3 Interface Friction Angle vs. Temperature**

When the temperature was increased from 0°C to 33°C, the peak interface friction angle increased for smooth gemembrane/NWNP geotextile and for textured gemembrane/NWNP geotextile from 12° to 14° degrees and from 25 to 27°, respectively (Fig. 4.5). The residual friction angles for these interface increases went from 11 to 13° and from 24 to 26° respectively. Tables 4.1 and 4.2 show the ratio of



(a)



(b)

Figure 4.5. Effects of temperature on interface friction angle: (a) textured geomembrane/NWNP geotextile, and (b) smooth HDPE geomembrane/NWNP geotextile.

interface friction angle obtained at various temperature to interface friction angles obtained at room temperature. Tables 4.3 and 4.4 shows the ratio of  $\tan\phi$ .

#### **4.3.4 Comparison With Other Data**

Tables 4.5 and 4.6 show a comparison between the interface friction angles, at room temperature, obtained from this research program and others. The friction angles are similar, except those measured by Stark et al. (1996).

#### **4.4 RELAXATION and ELONGATION**

To assess whether relaxation affects interface strength, additional tests were conducted 6 hours after the constant temperature was obtained and the normal stress was applied. The friction angle obtained from this second group of tests was  $0.5^\circ$  higher than the friction angle obtained from the tests conducted immediately after temperature equilibration (Fig. 4.6).

The length of each specimen was also measured before and after shear testing to determine if they elongated. No significant elongation was found for the geomembranes for all temperatures. Elongation of the NWNP geotextile specimens was greatest (3 mm to 5 mm) at a normal stress of 49 kPa and temperature of  $33^\circ\text{C}$  when tested with textured geomembrane, and minimum (1mm to 1.5 mm) at a normal stress of 7 kPa at  $0^\circ\text{C}$  when tested with smooth geomembrane. This suggests that greater elongation occurs at higher temperature.

Table 4.1. Friction Angles for NWNP Geotextile/Smooth HDPE Geomembrane.

$\phi/\phi_{(T=21^{\circ}\text{C})}$	$\phi_{(T=0^{\circ}\text{C})}/\phi_{(T=21^{\circ}\text{C})}$	$\phi_{(T=10^{\circ}\text{C})}/\phi_{(T=21^{\circ}\text{C})}$	$\phi_{(T=33^{\circ}\text{C})}/\phi_{(T=21^{\circ}\text{C})}$
PEAK	0.90	0.96	1.02
RESIDUAL	0.87	0.88	1.01

Table 4.2. Friction Angles for NWNP Geotextile/Textured HDPE Geomembrane

$\phi/\phi_{(T=21^{\circ}\text{C})}$	$\phi_{(T=0^{\circ}\text{C})}/\phi_{(T=21^{\circ}\text{C})}$	$\phi_{(T=10^{\circ}\text{C})}/\phi_{(T=21^{\circ}\text{C})}$	$\phi_{(T=33^{\circ}\text{C})}/\phi_{(T=21^{\circ}\text{C})}$
PEAK	0.95	0.96	1.03
RESIDUAL	0.92	0.95	1.01

Table 4.3  $\text{Tan}\phi$  for NWNP Geotextile/Smooth HDPE Geomembrane Interface

$\text{Tan}\phi/\text{Tan}\phi_{(T=21^\circ\text{C})}$	$\text{Tan}\phi_{(T=0^\circ\text{C})}/\text{Tan}\phi_{(T=21^\circ\text{C})}$	$\text{Tan}\phi_{(T=10^\circ\text{C})}/\text{Tan}\phi_{(T=21^\circ\text{C})}$	$\text{Tan}\phi_{(T=33^\circ\text{C})}/\text{Tan}\phi_{(T=21^\circ\text{C})}$
PEAK	0.9	0.96	1.03
RESIDUAL	0.87	0.89	1.02

Table 4.4  $\text{Tan}\phi$  for NWNP Geotextile/Textured HDPE Geomembrane Interface

$\text{Tan}\phi/\text{Tan}\phi_{(T=21^\circ\text{C})}$	$\text{Tan}\phi_{(T=0^\circ\text{C})}/\text{Tan}\phi_{(T=21^\circ\text{C})}$	$\text{Tan}\phi_{(T=10^\circ\text{C})}/\text{Tan}\phi_{(T=21^\circ\text{C})}$	$\text{Tan}\phi_{(T=33^\circ\text{C})}/\text{Tan}\phi_{(T=21^\circ\text{C})}$
PEAK	0.93	0.956	1.03
RESIDUAL	0.91	0.95	1.02

Table 4.5 NWNP Geotextile/Smooth HDPE Geomembrane Interface Shear Friction Angles at Room Temperature (21°C).

	This Study	Gilbert et al.	Pasqualini et. al.	Stark et al.	PGI/PVC G. Inst.	Bhatia et. al.
Device	TDISD	TDISD	Direct Shear	Ring Shear	Direct Shear	Direct Shear
Peak	14	~13	N.A.	~7.5	14	14
Residual	13	~10	12~14	~6	N.A.	N.A.

N.A. : Not Available.

Table 4.6 NWNP Geotextile/Textured Geomembrane Interface Friction Angles at Room Temperature (21°C).

	This Study	Stark et al.	PGI/PVC G. Inst.	Bhatia et. al.
Device	TDISD	Ring Shear	Direct Shear	Direct Shear
Peak	27	32	28	17
Residual	26	~17	N.A.	N.A.

N.A. : Not Available.

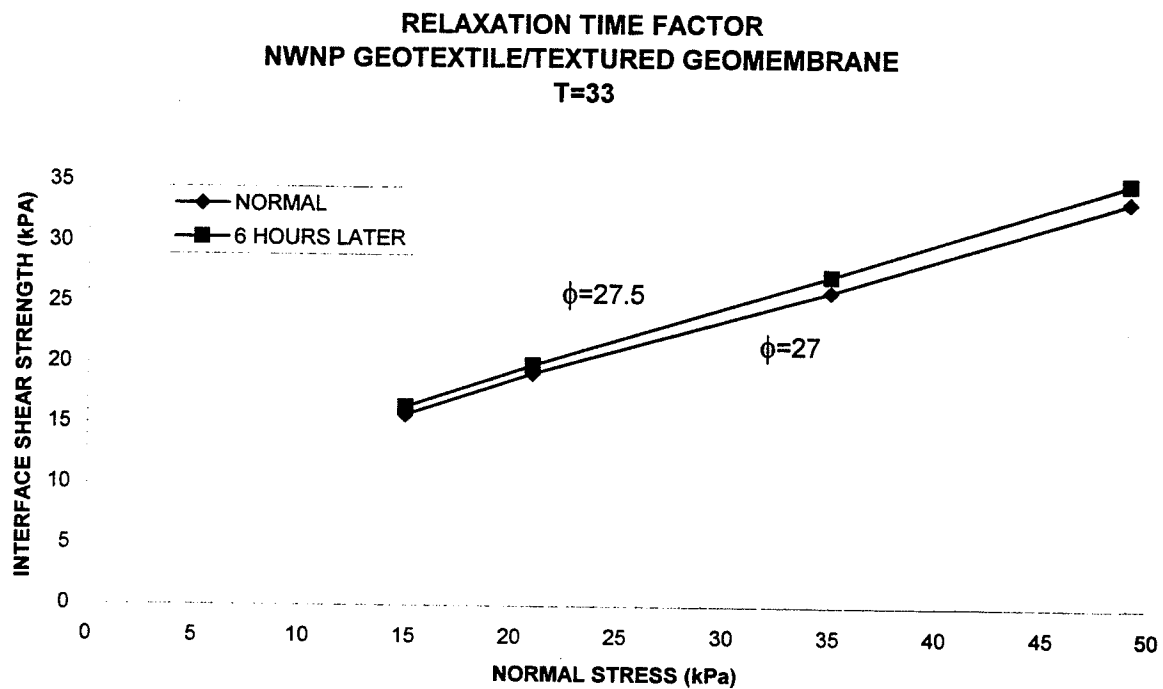


Figure 4.6. Relaxation Time Factor at T=33°C.

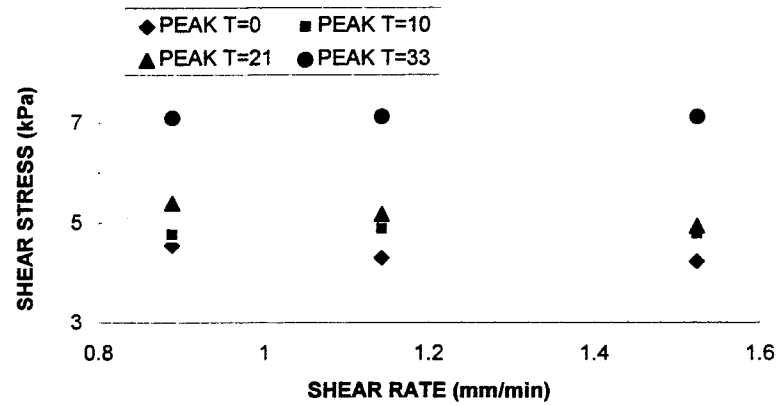
#### **4.5 EFFECT OF SHEAR RATE AT VARIOUS TEMPERATURES**

Stark et al. (1996) showed that shear displacement rate does not significantly affect the peak and residual shear stress for a textured geomembrane/NWNP geotextile interfaces tested at room temperature. Tests were conducted at a normal stress of 96 kPa and at shear rates from 0.03 to 35 mm/min. The peak and residual shear strengths varied little as the displacement rate ranged from 0.029 to 36.7 mm/min. Bove (1990) also showed that interface shear strengths in dry conditions are not sensitive to shear rate.

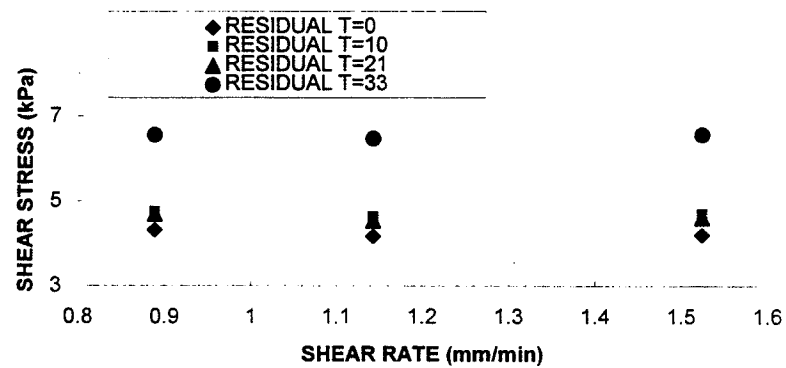
To assess whether similar results would be obtained at higher temperatures, tests were conducted at rates of 1.1, 0.9 mm/min, 1.5 mm/min at various temperatures (0°C, 10°C, 21°C, 31°C). Results of the tests are shown in Figs. 4.7 and 4.8. The peak and residual shear strength vary little with the shear rate, regardless of temperature. Based on this data, it appears that the shear displacement rate does not significantly affect the measured peak and residual shear stresses for temperatures encountered in landfill application.

#### **4.6 EFFECT OF MOISTURE**

Moisture on the specimen surfaces was expected when tests were conducted under cold conditions. Before and after each test, however, specimen surfaces were inspected but no moisture was found. The specimens weights before and after the tests were calculated; any difference would have indicated a potential gain or loss of water. The weight of the specimens before the tests were measured under normal

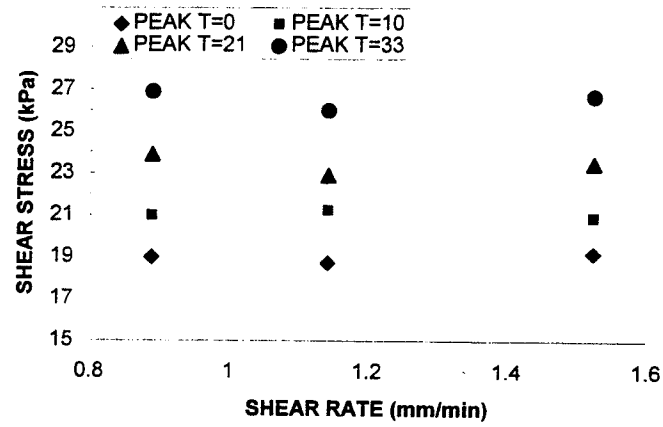


a) Peak

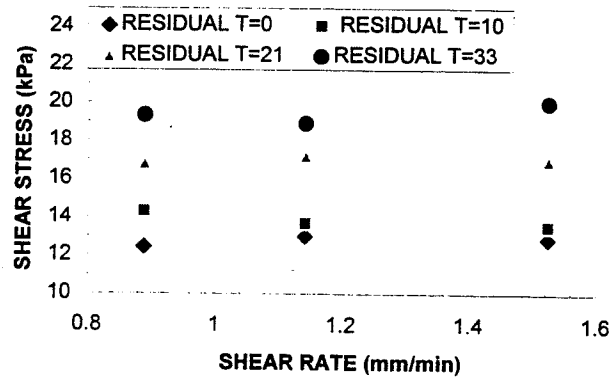


b) Residual

Figure 4.7 Effect of shear displacement rate on interface strength for smooth HDPE geomembrane/NWNP geotextile at  $\sigma=21$  kPa at different temperatures: (a) peak, (b) residual



a) Peak



(b) Residual

Figure 4.8 Effect of shear displacement rate on interface strength for textured HDPE geomembrane/NWNP geotextile at  $\sigma=21$  kPa at different different temperatures: (a) peak, (b) residual

room temperature (21°C). It was observed that the geomembrane (textured and smooth) surfaces were covered with thin water layer, when the specimens were kept in the refrigerator (below 0°C) for 2 hours. This suggested that if the interface shear strengths were conducted at temperatures below 0°C, lower interface shear strength results could have been obtained.

#### **4.7 OBSERVATION AT HIGH TEMPERATURES ON THE SPECIMENS BEFORE SHEARING**

Before conducting the interface shear tests, specimens of the geomembranes and geotextile were subjected to higher temperatures (33°C to 100°C). The specimens were observed under the microscope. The textured and smooth geomembrane surfaces became concave (or convex), and the geotextile fibers deformed (much like singed hair) and became sticky.

## SECTION FIVE

### SUMMARY AND CONCLUSIONS

Geosynthetics used in liners and covers undergo seasonal temperature changes. This study was conducted to assess whether these temperature changes affect interface shear strengths. For this purpose, a box was designed and used for maintaining constant temperature conditions (0°C to 33°C) during shear testing. A Texas double interface shear device was used for testing.

Variations in the testing program were temperature (0°C to 33°C), normal stress (15 to 49 kPa), geosynthetic type (1.5 mm smooth HDPE, impingement textured geomembrane, NWNP geotextile), and application time for the normal stress. Temperatures between 0°C and 33°C were used to represent field conditions measured in landfill caps. Tests conducted at low normal stress (<15 kPa) were not reliable due to friction problems in the shear machine.

Based on the results obtained from this study, the following conclusions are drawn:

1. The interface friction angle increases with increasing temperature. When the temperatures were increased from 0°C to 33°C, the peak interface friction angle increased for smooth gemembrane/NWNP geotextile and for textured gemembrane/NWNP geotextile from 12 to 14° and from 25 to 27°, respectively. The residual friction angles for these interface increases went from 11 to 13° and from 24 to 26°, respectively.

2. The interface shear strength increases with increasing temperature. When the temperatures were increased from 0°C to 33°C, the interface shear strength increased for smooth geomembrane/NWNP geotextile and for textured geomembrane/NWNP geotextile 20-68 % and 6-8.4 %, respectively, for peak values and 19.3-94 % and 0.77-6.45 %, respectively, for residual values.
3. At various temperatures, textured geomembranes had interface friction angles two times higher than their smooth counterparts.
4. Relaxation time has an effect on the interface friction angle. The friction angle obtained from tests conducted at 33°C 6 hours after the equilibrium temperature was obtained were 0.5° higher than the friction angle obtained immediately after the equilibrium temperature was obtained.
5. Shear rate does not have a significant effect on the interface shear strength, regardless of temperature.

## REFERENCES

- ASTM (1991), "Standard Test Method for Measuring Nominal Thickness of Geotextiles and Geomembranes," ASTM Standard No. D 5199-91, *Annual Book of ASTM Standards*.
- ASTM (1992a), "Standard Terminology for Geosynthetics," ASTM Standard No. D 4439-92, *Annual Book of ASTM Standards*.
- ASTM (1992b), "Standard Test Method for Measuring Mass Per Unit Area of Geotextiles," ASTM Standard No. D 5261-92, *Annual Book of ASTM Standards*.
- ASTM (1992c), "Standard Test Method for Determining the Coefficient of Friction of Soil and Geosynthetic or Geosynthetic and Geosynthetic Friction by the Direct Shear Method," ASTM Standard No. D 5321-92, *Annual Book of ASTM Standards*.
- Bely, V. A., Sviridenok, A. I., Petrokovets, M. I., Savkin, V. G. (1982), "Friction & Wear In Polymer-Based Materials Granville P.-Jackson ed., Peramon Press Inc., New York.
- Bove, J. A. (1990), "Direct Shear Friction Testing For Geosynthetics in Waste Containment," *Geosynthetic Testing for Waste Containment Applications, ASTM STP 1081*, Robert M. Koerner, editor, American Society for Testing and Materials, Philadelphia.
- Byrne, R., Kendall, J., and Brown, S. (1992), "Cause and Mechanism of Failure, Kettleman Hills Facility, Kettleman City, California", Report Prepared for Chemical Waste Management, Inc. by Geosyntec Consultants, Atlanta, Georgia.
- Cadwallader, M., Cranston, M., Peggs, I. D. (1993), "White-Surfaced HDPE Geomembranes: Assessing Their Significance to Liner Design and Installation," *Proc. Geosynthetics '93*, Vancouver, Canada. pp. 1065.
- Corser, P., M. Cranston (1991), "Observations on Long-Term Performance of Composite Clay Liners and Covers," *Proceedings, Geosynthetic Design and Performance*, Vancouver Geotechnical Society, Vancouver, British Columbia.

- Daniels, C. A. (1989), *Polymers: Structure and Properties*, Technomic Publishing Company, Inc., Lancaster, Pennsylvania.
- Gahr, K. H. Z (1987), "Microstructures And Wear Of Materials", Elsevier Science Publishing Company Inc., New York, N. Y.
- Gilbert, R. B., Liu, C. N., Wright, S. G., Trautwein, S. J. (1995), "A Double Interface Test Method for Measuring Interface Strength," *Proc. Geosynthetics '95 Conference*, Nashville, Tenn. pp. 1017-1029.
- Khire, M. V. (1994), "Final Cover Hydrologic Evaluation," Environmental Geotechnics Report 94-4, Dept. of Civil and Environmental Engineering, University of Wisconsin-Madison.
- Koerner, R. M. (1994), *Designing with Geosynthetics, 3<sup>rd</sup> edition*, Prentice-Hall Englewood Cliffs, N.J.
- Montgomery, Robert J., and Parsons, Laurie J., (1990), "The Omega Hills Final Cover Test Plot Study; Three-Year Data Summary," *EPA Seminars-Design and Construction of RCRA/CERCLA Final Covers*, Oakland, California.
- Nielsen, L. E. and Landel, R.F. (1994), *Mechanical Properties of Polymers and Composites*, Marcel Dekker, Inc., New York, N.Y.
- O'Rourke, T.D. Druschel, S.J., and Netravali, A.N., (1990), "Shear Strength Characteristics of Sand Polymer Interfaces," *Journal of Geotechnical Eng.*, ASCE, Vol.116, No.3, pp. 451-469.
- Osswald, T. A. and Menges, G. (1995), *Materials Science of Polymers for Engineers*, Hanser/Gardner Publications, Inc., Cincinnati.
- Pasqualini, E., Sani, D., and Roccato, M. (1993), "Factors Influencing Geomembrane Interface Friction," *Waste Disposal by Landfill Green'93*, R.W. Sarsby ed., Bolton Institute of Higher Education, United Kingdom, pp. 349-356.
- Scranton, H. B. (1996), "Field Performance of Sloping Test Plots Containing Geosynthetic Clay Liners," *M.S. Thesis*, University of Texas, Austin, Texas.
- Stark, T. D., and Poeppel A. R. (1994) "Landfill Liner Interface Strengths from Torsional-Ring-Shear Tests," *J. of Geotechnical Eng.*, Vol. 120, No 3., pp. 597-615.

Stark, T. D., Williamson, T. A., and Eid, H. T. (1996) "HDPE Geomembrane/Geotextile Interface Shear Strength," *J. of Geotechnical Engineering*, Vol, 122, No. 3., pp. 197-203.

Tisinger, L. G., Peggs, I. D., Dudzik, B. E., Winfree, J. P., and Carraher, Jr., C. E., (1990), "Microstructural Analysis of a Polypropylene Geotextile After Long-Term Outdoor Exposure", *Geosynthetic Testing for Waste Containment Applications, ASTM STP 1081*, Robert M. Koerner, ed., American Society for Testing and Materials, Philadelphia, pp. 335-351.

**APPENDIX A**

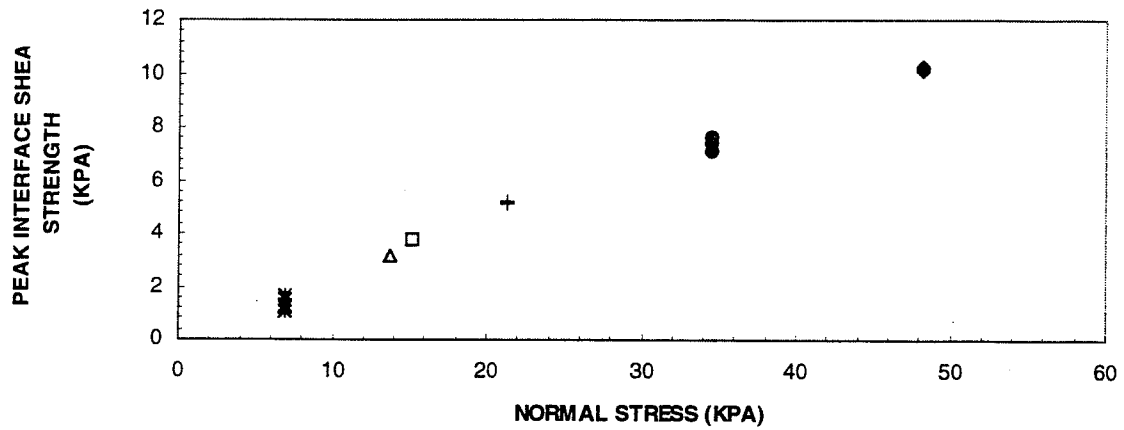
**NWNP GEOTEXTILE/TEXTURED GEOMEMBRANE**

**AND**

**NWNP GEOTEXTILE/SMOOTH GEOMEMBRANE**

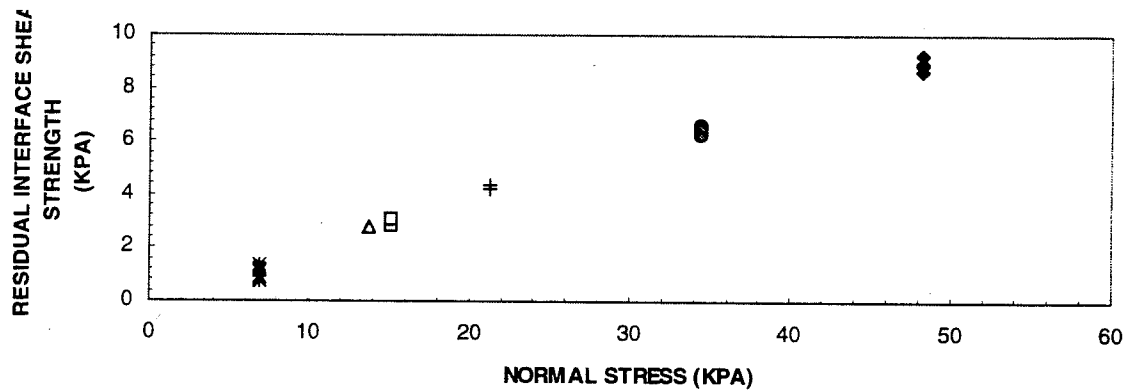
**GRAPHS**

PEAK INTERFACE SHEAR STRENGTH V.S. NORMAL STRESS  
(NONWOVEN NEEDLE PUNCHED GEOTEXTILE- 60 MIL HDPE)  
at T=21



(a)

RESIDUAL INTERFACE SHEAR STRENGTH V.S. NORMAL STRESS  
(NONWOVEN NEEDLE PUNCHED GEOTEXTILE- 60 MIL HDPE)  
at T=21



(b)

Figure A.1. Repeatable Interface Shear Strength Results at T=21 °C : (a) peak, and (b) residual.

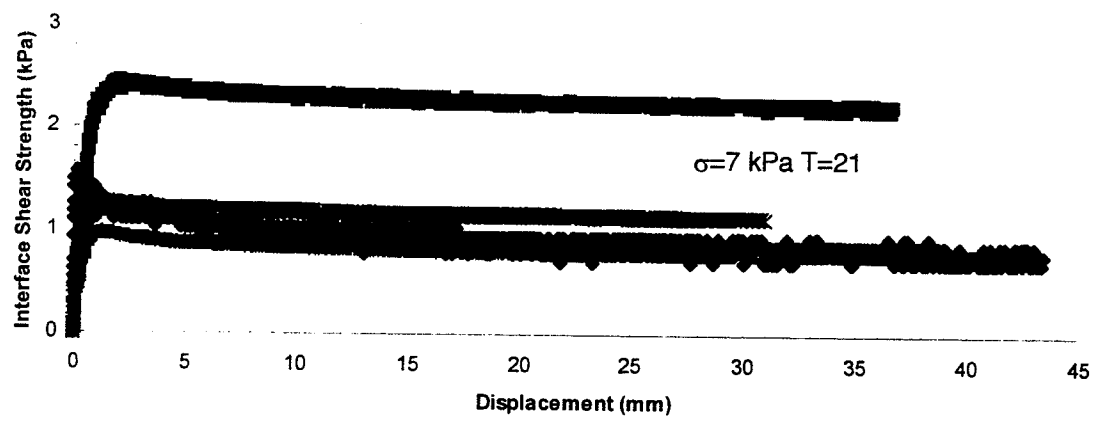


Figure A.2. Interface Shear Strength vs. Displacement  $\sigma=7$  KPA at  $T=21^{\circ}\text{C}$ .

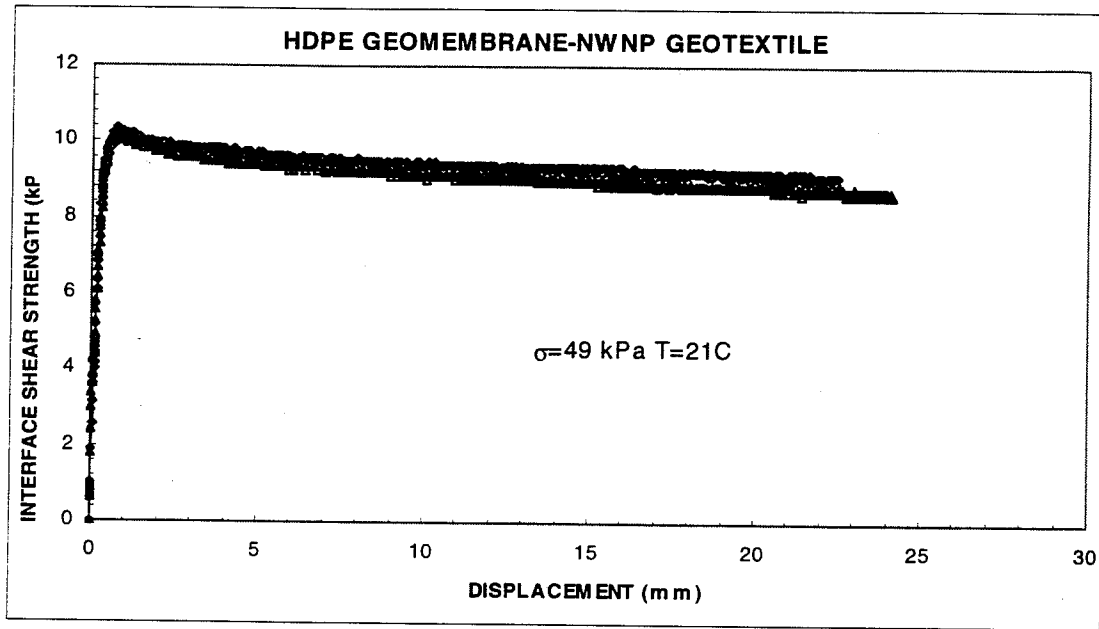
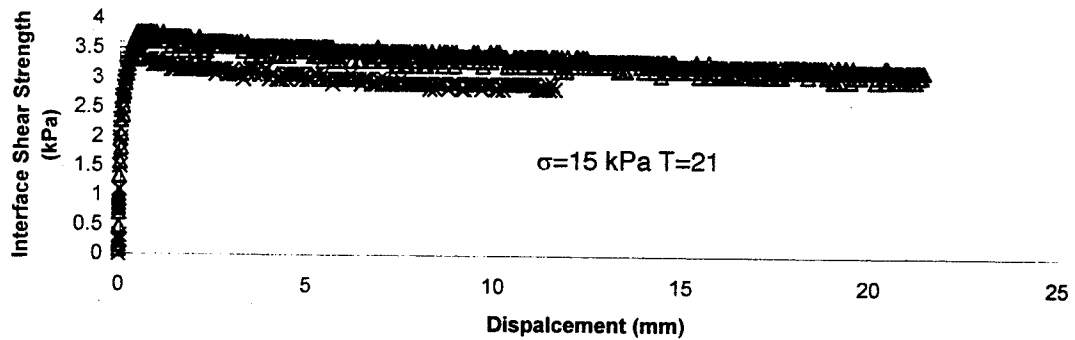


Figure A.3. Interface Shear Strength Results Above  $\sigma = 7 \text{ kPa}$  at  $T = 21^\circ\text{C}$

## HDPE GEOMEMBRANE-NWNP GEOEXTILE



## HDPE GEOMEMBRANE-NWNP GEOEXTILE

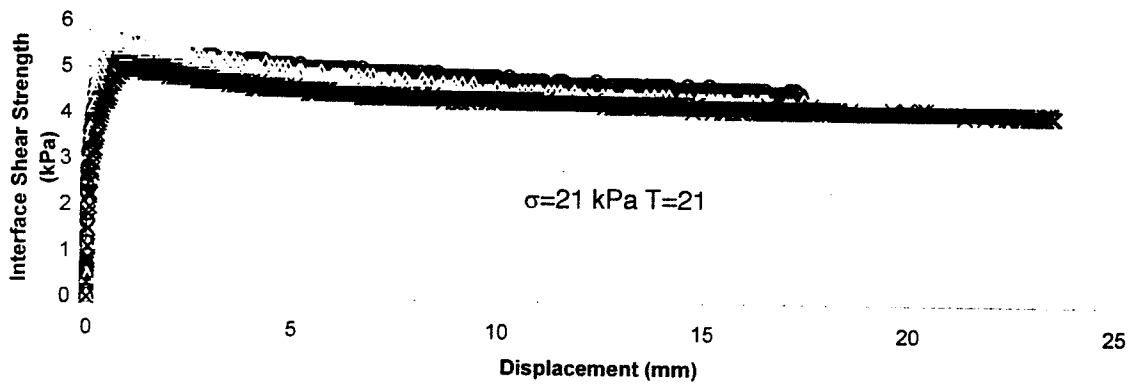


Figure A.4. Interface Shear Strength vs. Displacement Above  $\sigma=7 \text{ kPa}$  at  $T=21^\circ\text{C}$ .

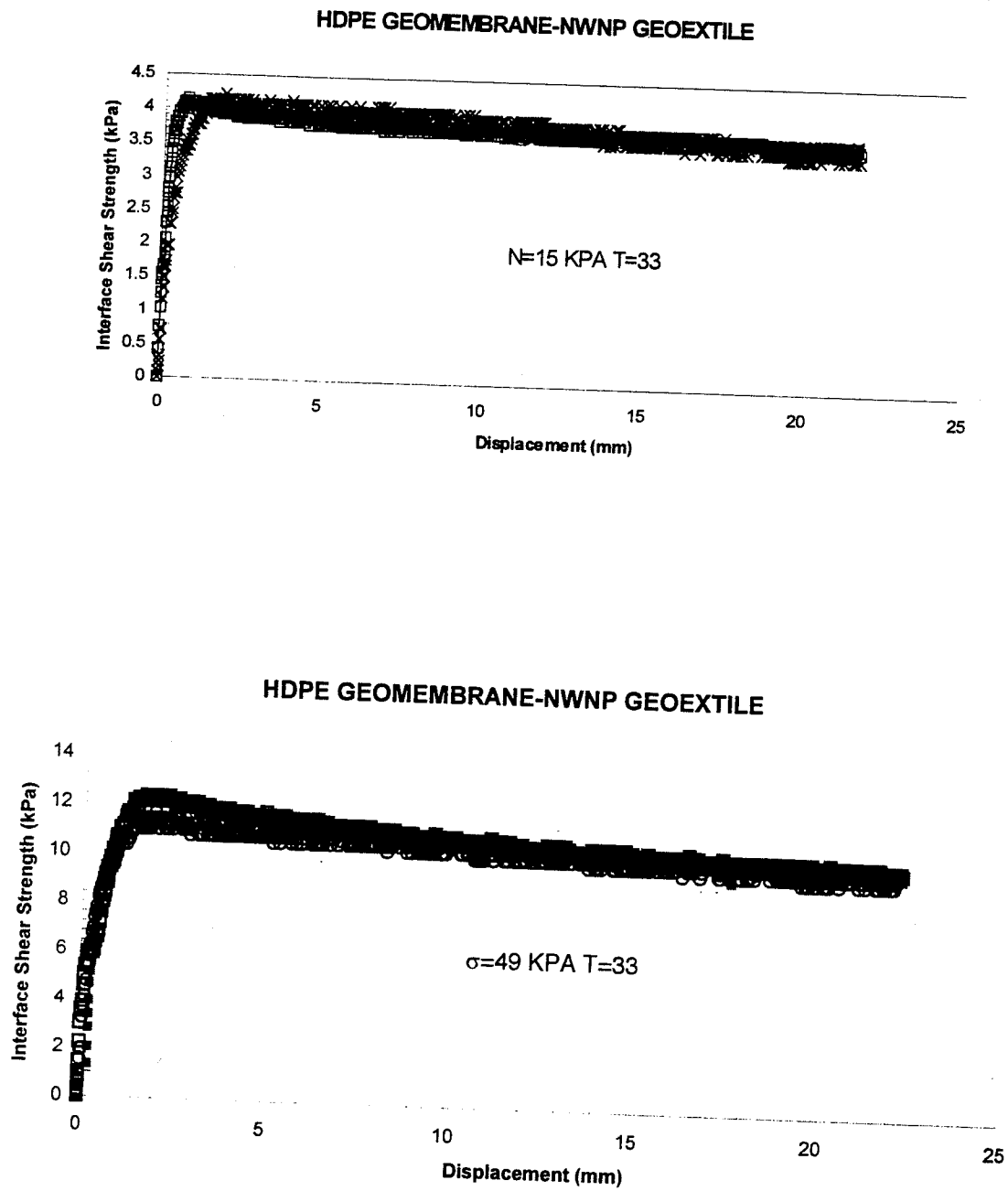


Figure A.5. Interface Shear Strength vs. Displacement Above  $\sigma=7$  kPa at  $T=33^{\circ}\text{C}$ .

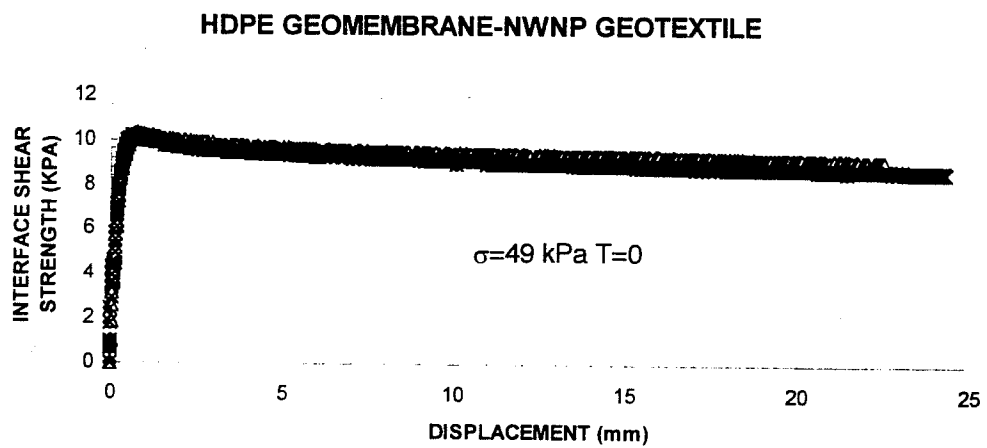
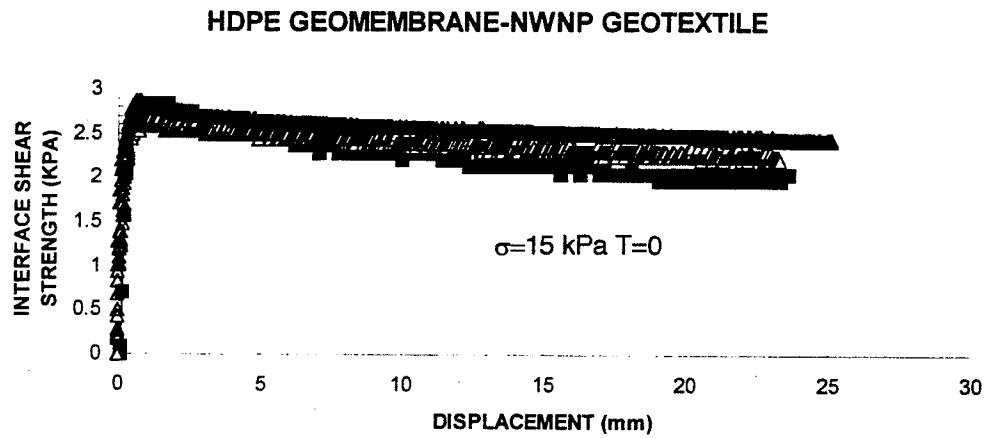


Figure A.6 Interface Shear Strength vs. Displacement Above  $\sigma=7 \text{ kPa}$  at  $T=0^\circ\text{C}$ .

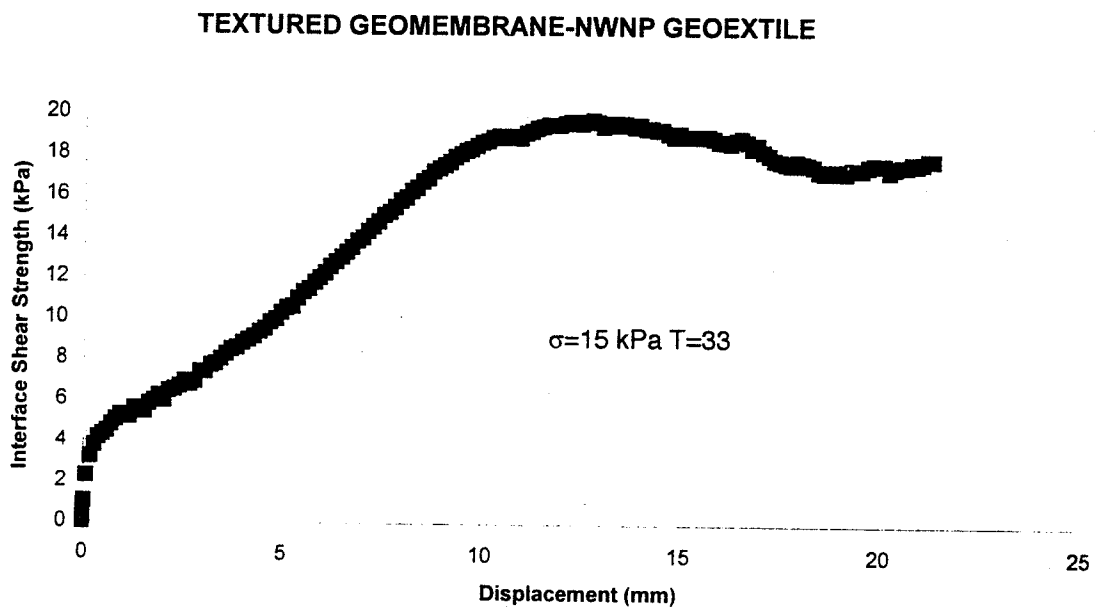
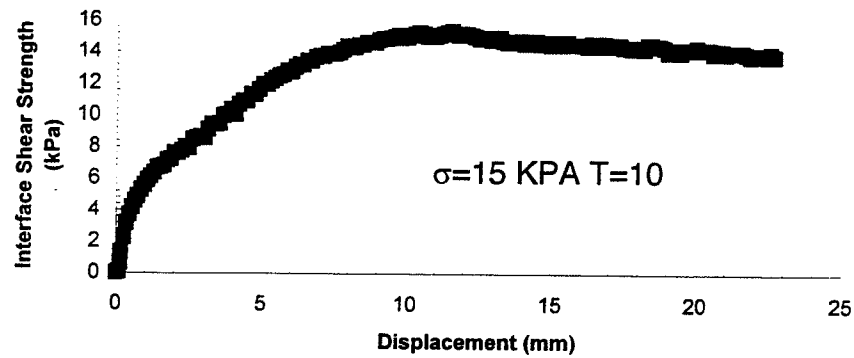


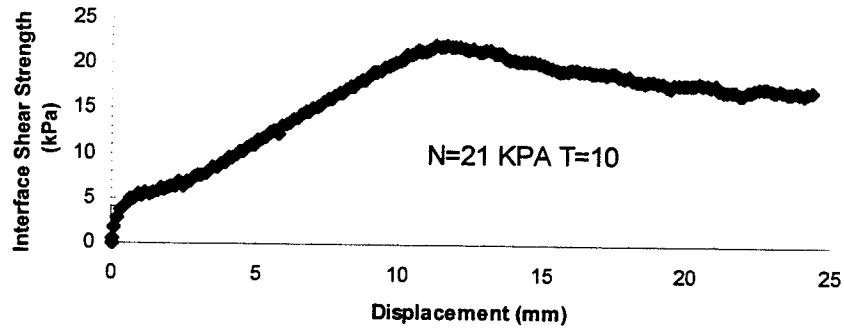
Figure A.7. Interface Shear Strength vs. Displacement Above  $\sigma=15 \text{ kPa}$  at  $T=33^\circ\text{C}$ .

## TEXTURED GEOMEMBRANE-NWNP GEOEXTILE



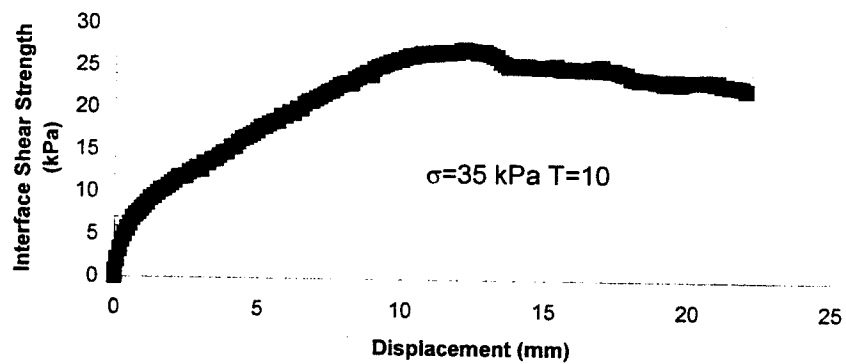
(a)

## TEXTURED GEOMEMBRANE-NWNP GEOEXTILE



(b)

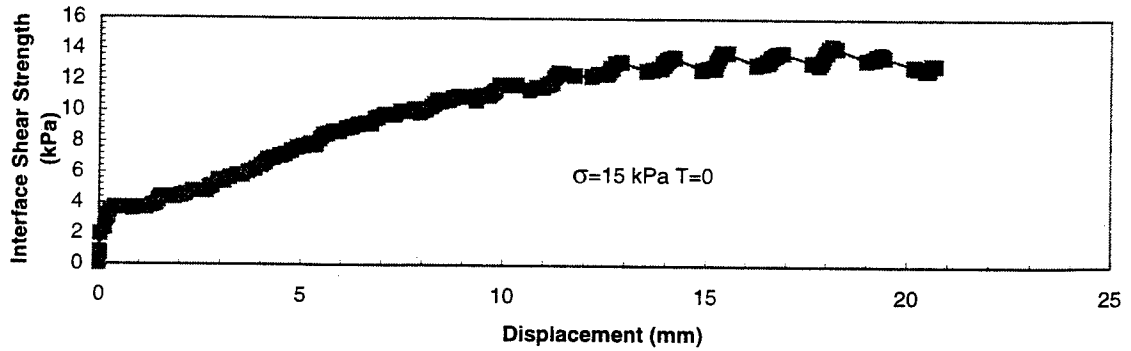
## TEXTURED GEOMEMBRANE-NWNP GEOEXTILE



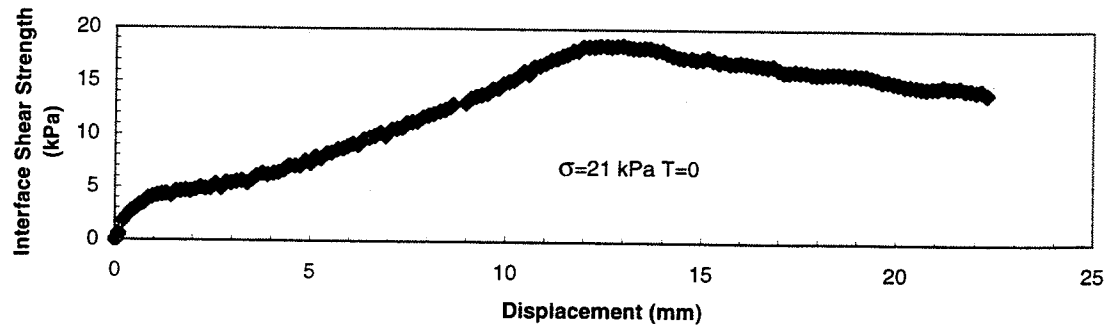
(c)

Figure A.7. Interface Shear Strength vs. Displacement at  $T = 10^\circ\text{C}$ .

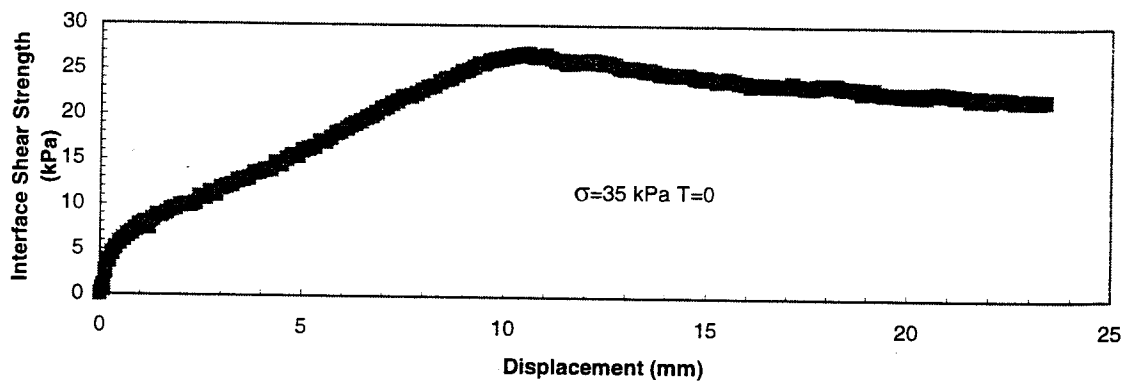
## TEXTURED GEOMEMBRANE-NWNP GEOEXTILE



## TEXTURED GEOMEMBRANE-NWNP GEOEXTILE

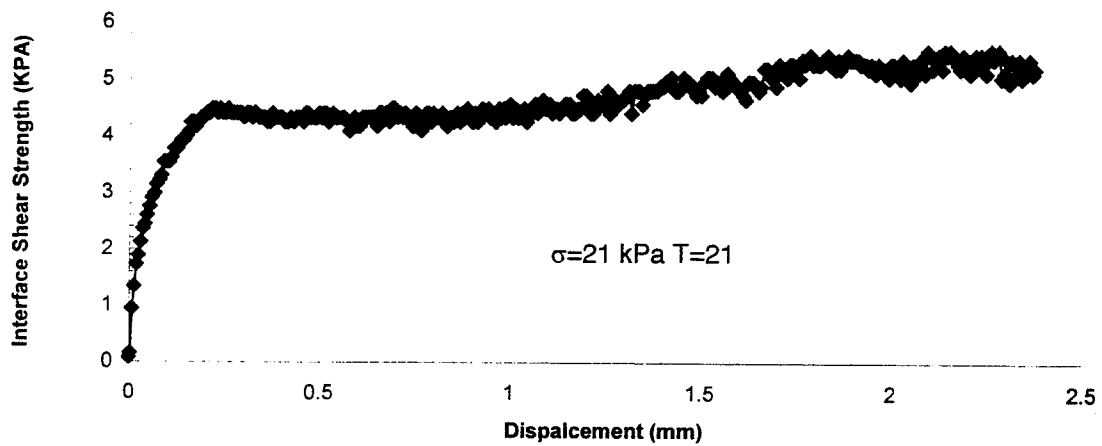


## TEXTURED GEOMEMBRANE-NWNP GEOEXTILE

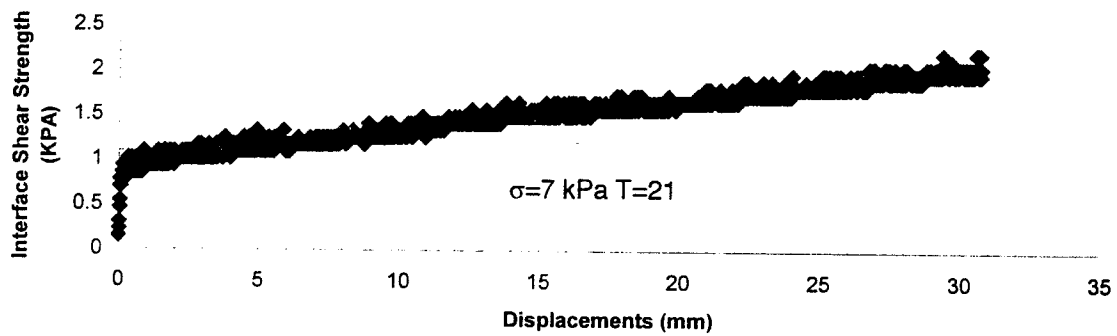
Figure A.3. Interface Shear Strength Results Above  $\sigma=7$  kPa at  $T=0^\circ\text{C}$ .

**APPENDIX B**

**ERRORS DURING SHEARING**



(a)



(b)

Figure B.1 When Aluminum Plates of the TDISD Were Not Maintained Parallel to Each Other : (a), (b) NWNP Geotextile/Smooth HDPE.

**APPENDIX C**

**CALIBRATION OF LOAD CELLS AT VARIOUS TEMPERATURES**

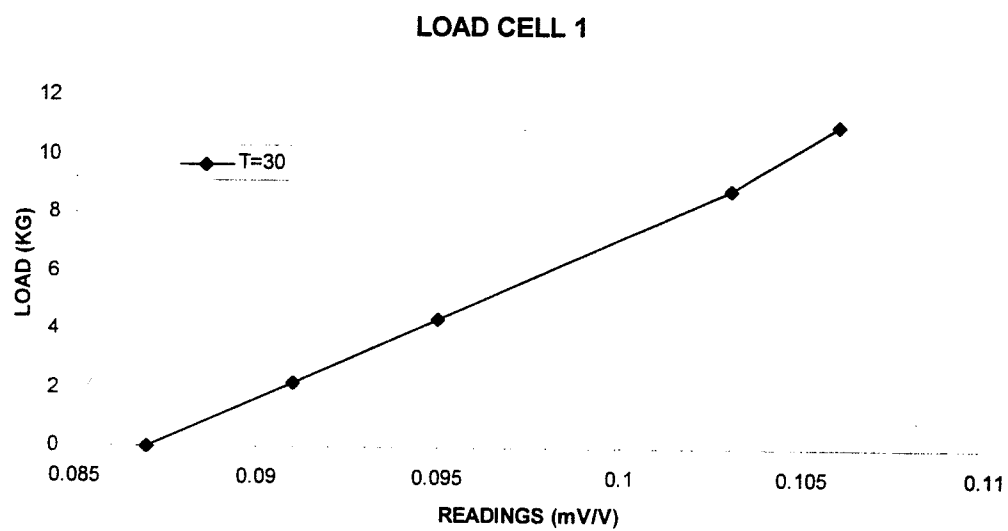
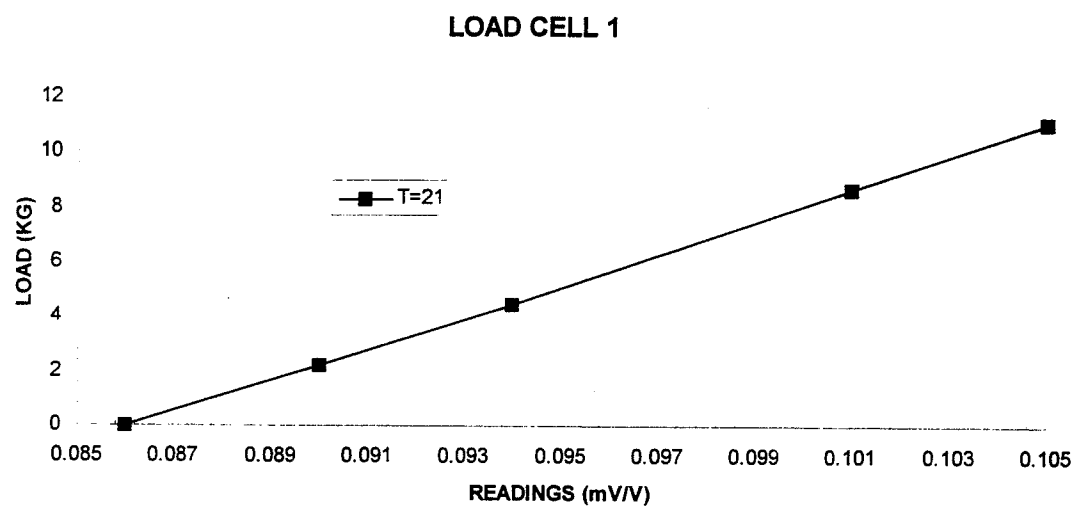


Figure C.1. Load Cell Calibration at Various Temperatures.

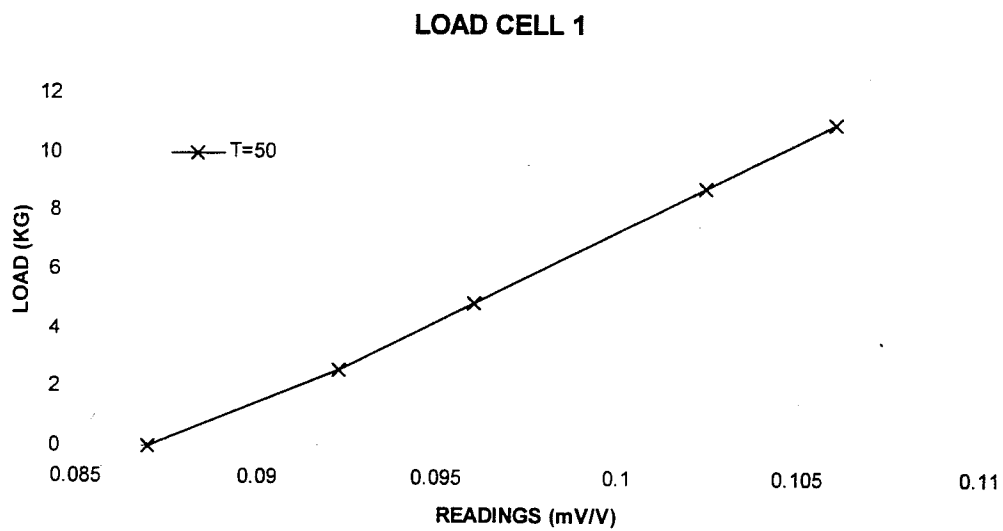
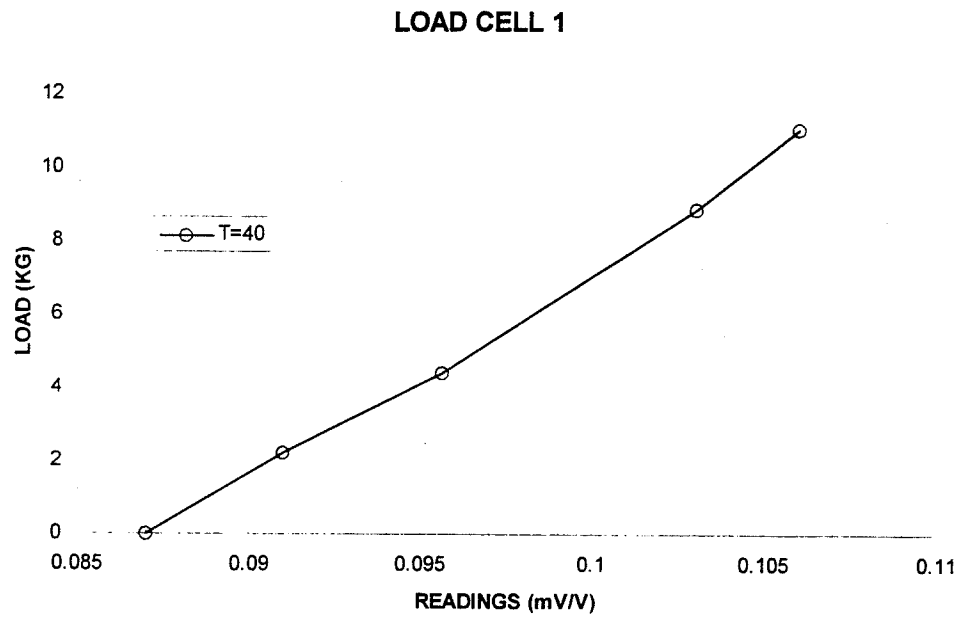


Figure C.2. Load Cell Calibration at Various Temperatures.

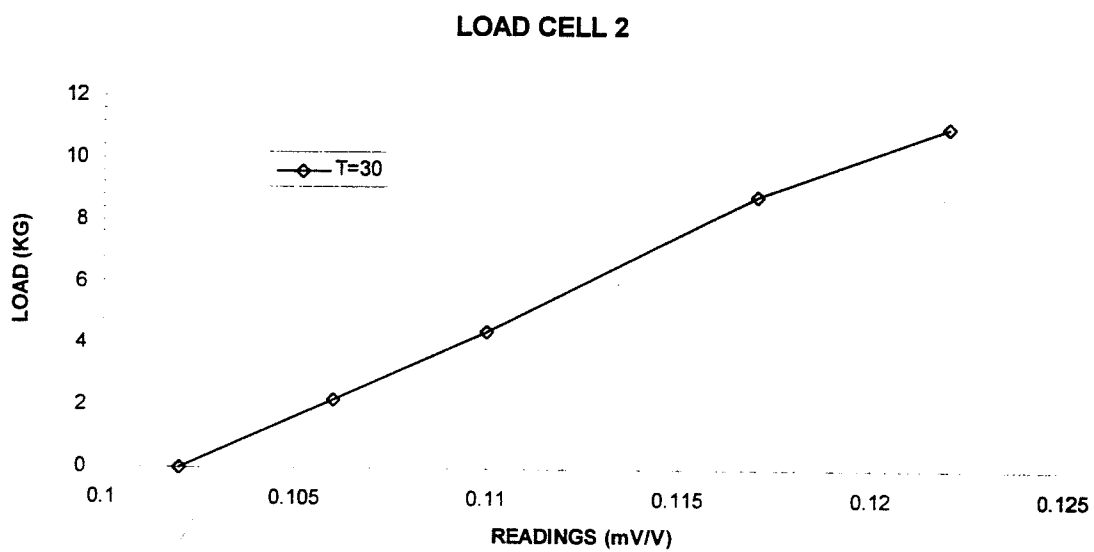
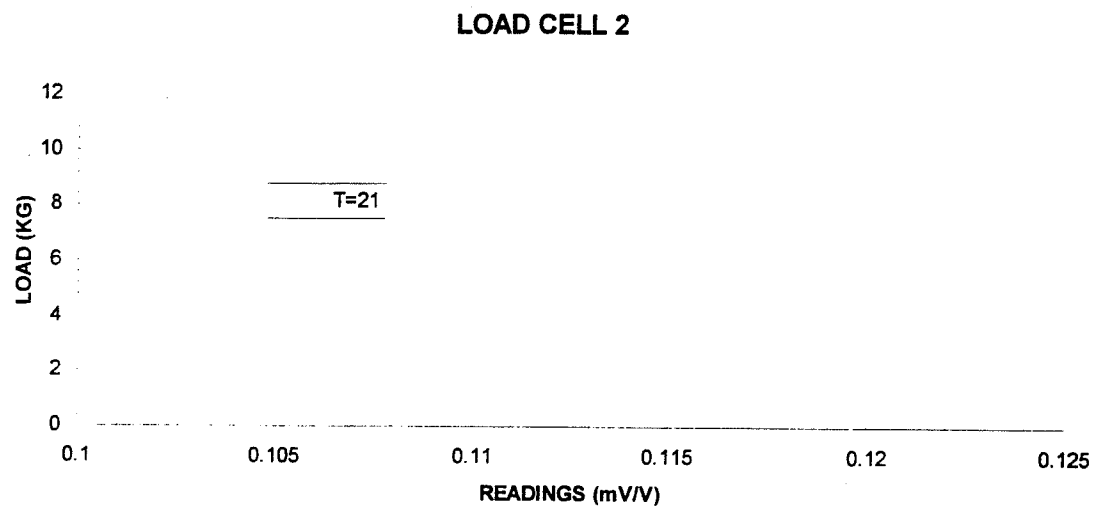


Figure C.3. Load Cell Calibration at Various Temperatures.

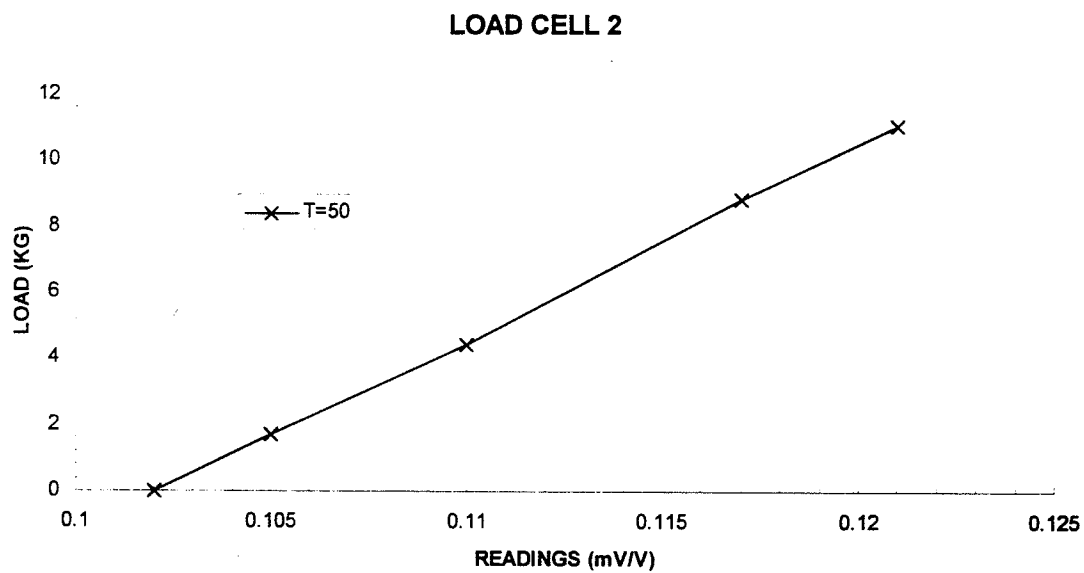
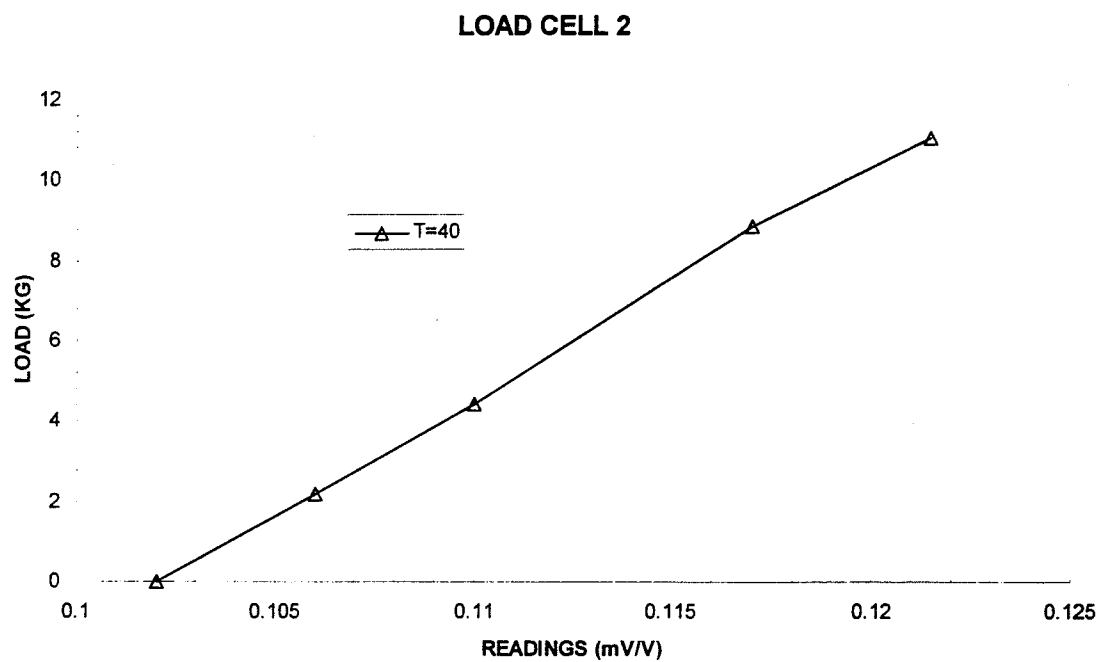


Figure C.4 Load Cell Calibration at Various Temperatures.